(19) Europäisches Patentamt
European Patent Office
Office européen des brevets

(11) **EP 4 328 286 A1**

(12) **EUROPEAN PATENT APPLICATION**

(43) Date of publication:
28.02.2024 Bulletin 2024/09

(21) Application number: **22306835.4**

(22) Date of filing: **09.12.2022**

(51) International Patent Classification (IPC):
C10B 19/00 $^{(2006.01)}$ ***C10B 53/07*** $^{(2006.01)}$
C10G 1/10 $^{(2006.01)}$ ***H05B 6/10*** $^{(2006.01)}$

(52) Cooperative Patent Classification (CPC):
C10G 1/10; C10B 19/00; C10B 53/07; H05B 6/06; H05B 6/105

(84) Designated Contracting States:
AL AT BE BG CH CY CZ DE DK EE ES FI FR GB GR HR HU IE IS IT LI LT LU LV MC ME MK MT NL NO PL PT RO RS SE SI SK SM TR
Designated Extension States:
BA
Designated Validation States:
KH MA MD TN

(30) Priority: **25.08.2022 EP 22306251**

(71) Applicants:
- **Centre National de la Recherche Scientifique**
  75016 Paris (FR)
- **Université de Strasbourg**
  67000 Strasbourg (FR)
- **SICAT**
  75009 Paris (FR)
- **Blackleaf**
  67100 Strasbourg (FR)

(72) Inventors:
- **DUONG-VIET, Cuong**
  67400 Illkirch-Graffenstaden (FR)
- **PHAM, Charlotte**
  67000 Strasbourg (FR)
- **PHAM-HUU, Cuong**
  67100 Strasbourg (FR)
- **TRUONG-PHUOC, Lai**
  67200 Strasbourg (FR)
- **NHUT, Jean-Mario**
  67115 Plobsheim (FR)
- **BA, Housseinou**
  67000 Strasbourg (FR)
- **LAFUE, Yannick**
  67100 Strasbourg (FR)
- **WAMBERGUE, Stéphane**
  67000 Strasbourg (FR)

(74) Representative: **Novagraaf Technologies**
Bâtiment O2
2, rue Sarah Bernhardt
CS90017
92665 Asnières-sur-Seine Cedex (FR)

(54) USE OF A METAL-FREE CARBON MATERIAL FOR CONVERTING PLASTIC INTO C2-C4 OLEFINS AND/OR HYDROCARBONS, UNDER DIRECT INDUCTION HEATING, AND METHOD THEREOF

(57) The present invention refers to the use of a metal-free carbon material for converting plastic into C_2-C_4 olefins and/or other hydrocarbons, under direct induction heating at temperature less than or equal to 800 °C.

The present invention also relates to a process for converting plastic into C_2-C_4 olefin and/or other hydrocarbons, comprising a step of reaction under direct induction heating, with a metal-free carbon material as defined in anyone of the claims, at temperature less than or equal to 800 °C.

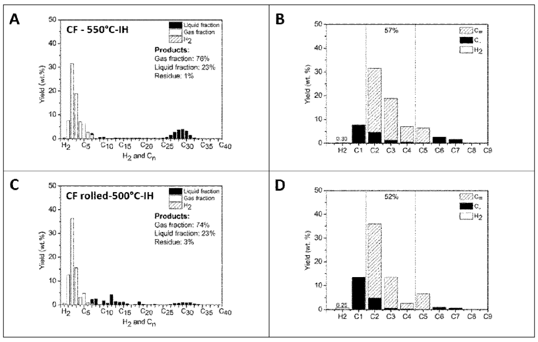

Figure 4

Processed by Luminess, 75001 PARIS (FR)

Description

Technical field

[0001] The present invention refers to the use of a material for converting plastic into C_2-C_4 olefins and/or other hydrocarbons, and to a process for converting plastic into C_2-C_4 olefin and/or other hydrocarbons.

[0002] Therefore, the present invention has utility in plastic and chemistry industry field, especially in recycling field.

[0003] In the description below, the references into brackets ([ ]) refer to the listing of references situated at the end of the text.

Background of the Invention

[0004] Plastics represent one of the main commodities for daily uses in almost every domain, spanning from industrial packaging to health care and composites for transport and storage. It has been estimated that about 380 million tons of petroleum-based plastics were produced in 2015. The majority of them are used in packaging (mostly as single-use), while the others ended up in construction, automotive, electrical devices, and many others applications. It has also been estimated that this amount is expected to double by 2035, taken into account the annual growth rate. The single-use of plastics (40 %) as commodities represents one of the main contribution to CO_2, causing problem for environmental and health as nowadays, about 90% of the waste plastic is dumped or landfilled while only a small amount is recycled. In addition, a large part of waste plastic is ending up in rivers and oceans, posing problems for natural environment.

[0005] New legislations and environmental pushes significantly contribute to the increase of waste plastic recycling to produce raw material for new plastics or liquid fuels for transportation and petrochemicals. The plastic-to-fuel (PTF) transformation has received an ever increasing academic but also industrial interest since the last years. Most recently, several announcements have been made by different industrials for new plants settling to convert waste plastics into valuable gaseous/liquids components which contribute to the renewable interest for such process.

[0006] Plastic waste as such is contaminated with other products and thus, preliminary sorting and cleaning are necessary before initiating the recycling process. Nowadays, depending on the quality and purity of the plastic waste, different processes for recycling can be used: (i) reuse (direct from the waste plastic), (ii) reprocessing or mechanical recycling, (iii) depolymerization to the raw monomeric material (not for all types of waste plastic), (iv) conversion of the waste plastic into hydrocarbon feedstock, and finally (v) energy recovery through incineration. The recycling efficiency also depends on the nature of the various additives present in the plastic.

[0007] The conversion of plastic to liquid or gaseous hydrocarbons also allows one to recycle solid waste fractions that cannot be reused or recycled through mechanical or depolymerization processes and to avoid landfill or incineration. Waste plastic recycling allows one to reduce in a significant manner the greenhouse gas (GHG) emission compared to incineration. Alongside with the conversion of waste plastic into liquid fuels, other researches also aim to convert such wastes into light olefins, which display high interest for base chemicals, i.e. raw monomers for plastics production. However, the direct conversion of waste plastics into light olefins is not a straightforward process and thus, indirect route is developed through converting waste plastics into intermediate hydrocarbons and further converting such chemicals into light olefins. Onwudili et al. (Onwudili et al., 2019 ([1])) investigated the conversion of polyolefin vapors from a mixture of plastics (HDPE, LDPE, PP, PS and PET) over FCC (Fluid Catalytic Cracking) with Y-zeolite at 500°C and ZSM-5 zeolite at 600°C. The amount of C_2-C_4 olefins obtained remains relatively low at ca. 21 wt%.

[0008] Depolymerization of polyolefins into their monomeric constituents, plastic-to-olefins (PTO) process, requires relatively harsh pyrolysis conditions and results in a complex mixture of hydrocarbons. In general, pyrolysis of polyolefin yields a mixture of paraffinic and olefinic waxes under moderate reaction conditions (450 °C) while more aromatics are produced at more severe conditions and finally, olefin-rich gas and char were produced at even more severe conditions ($\geq$ 700 °C) (Lopez et al., 2017 ([2]); Dogu et al., 2021 ([3])). In order to maximize the olefins fraction, the aliphatic compounds produced under mild conditions can be further processed into lower olefins through a steam cracker (FCC) which can produce a yield of 65 wt. % of olefins. The Synova technology is based on the use of hot fluidized sand bath to crack plastic wastes to produce liquid and tar which is further cracked to produce olefin-rich gas. Anellotech and BioBTX have developed pyrolysis using acid zeolites to convert the plastic pyrolysis vapors to lower olefins and waxes. However, catalyst deactivation requires complex reactor design and frequent catalyst regenerations (J.-P. Lange, Managing Plastic Waste-Sorting, Recycling, Disposal, and Product Redesign, ACS Sustain. Chem. Eng., 2021, 9, 15722-15738 https://doi.org/10.1021/acssuschemeng.1c05013 ([4])).

[0009] In addition, in order to reduce the GHG emissions of the chemical industry, it is highly desirable to replace the usual way of operating catalytic processes, i.e. with a combination of large gas burners and metal catalysts, by a brand new one. The replacement of natural gas burners by electrified heating systems has received a tremendous industrial interest since the last few years. For example, the recent consortium regrouping several petroleum industrials develops new steam crackers operating with electricity (Layritz et al., 2021 ([5])), electrocatalysis (Schiffer et al., 2017 ([6])) or with intermediate heating modes using electricity such as microwave, plasma or induction heating (Jie et al., 2020 ([7]); Zhou et al., 2021 ([8])). It is also desirable to replace traditional supported metal or zeolitic catalysts by metal-free ones with reduced production costs and environmental impacts. Last but not least, the ability to use electricity, directly or indirectly, to produce chemicals, also represents a smart way for storing excedental electrical energy from renewable sources, which could help to overcome the intermittency of energy produced from solar and wind.

[0010] Inductive heating (IH) has been widely developed in the manufacturing of industrial metallic work pieces (bonding, welding, sintering) in several industries. The heat is generated directly inside the targeted material and thus, it significantly reduces the energy lost by conduction or thermal radiation (Wang et al., 2019 ([9])). In such processes, the heat can be directed inside the interest area without over heating the whole large volume of the oven. For catalytic processes, it can thus avoid thermal decomposition of the reactants and products that would form unwanted amorphous carbon. Recently, IH mode has been reported as an efficient heating mode for operating catalytic processes with significant improved performance (Wang et al., 2019 ([9])). Alongside with the advantages cited above, IH also represents a green heating mean for operating catalytic processes as it can be operated using exceeding renewable energy (RE) sources, instead of using traditional fuel burner for providing heat to the reactor, which contributes to the reduction of CO_2 for the process. The faster heat generation in the system could also reduce energy loss generated during long start-up when using traditional indirect heating mode. The rapid quenching of the exit gaseous effluent, due to the targeted heating of IH, also reduces in a significantly way the cost of the process by suppressing cooling system at the exit of the catalytic section.

[0011] The most commonly used catalysts, for either PTF or PTO (plastic-to-olefin) transformation, are based on acidic zeolites, i.e. ZSM5, USY, which are operated through acidic cracking to generate liquid or gaseous hydrocarbons from pyrolysis polymer vapors. A recent study also pointed out the use of acid carbon-based catalysts for converting industrial waste plastics into jet fuel (Y. Zhang, D. Duan, H. Lei, E. Villota, R. Ruan. Jet fuel production from waste plastics via catalytic pyrolysis with activated carbons. Appl. Energy 251, 113337 (2019)).

[0012] However, a need exists for an alternative method that is easy to use, highly selective and energy efficient. The present invention fulfills these and other needs.

Description of the invention

[0013] The Applicant has surprisingly found that a metal-free carbon material can be used for PTF and PTO processes.

[0014] More particularly, the Applicant surprisingly reports on the combination use of metal-free carbon material and direct induction heating at medium temperature, to directly convert waste plastics into light olefins, especially ethylene and propylene, or into other hydrocarbons such as liquid hydrocarbons, especially fuel, and/or paraffinic gaseous C_1 to C_5 hydrocarbons.

[0015] The metal-free carbon materials used in the invention are particularly advantageous due to their high resistance towards deactivation in the presence of impurities contained in the waste plastics, and also to their low cost of production compared to the other materials.

[0016] Advantageously, the high chemical inertness of these carbon-based materials could also allow one to carry on a regeneration process through chemical treatment in order to remove the deposited impurities.

[0017] In addition, carbon-based materials are active for being heated up through direct induction heating, which open new paths for the development of electrification of processes for the recycling of waste plastics.

[0018] The combination of carbon-based materials and induction heating presents several advantages as discussed below.

[0019] An advantage of using induction heating is that it can be applied to fixed bed configuration as the heat is homogeneously generated on the outer surface of the carbon by eddy currents resulting from the interaction between the carbon-based material and the magnetic field. The high thermal conductivity of such carbon-based materials also contributes to the high heat transfer within the solid bed which, combined with the high heating rate, will allow one to maintain the bed temperature during the highly endothermic PTF or PTO process. It is very advantageous compared to prior art heating methods, for example microwave (MW) heating. In a fixed bed, the particles are in contact with each other and have high heat absorption next to the MW antenna. Thus, only a small area around the MW antenna is heated which generate local hot spot which could modify the selectivity of the process. In order to disperse the heat among the whole reaction section, a fluidization is needed to provide a homogeneous heat distribution. The use of fluidized bed induces an excess of energy consumption for moving the material and it also generates fines, through catalyst attrition, which could affect the material integrity.

[0020] Another advantage is that the invention may be realized as a two-stage process, i.e. waste plastic vaporization in a first-stage reactor, while the plastic vapors are swept with an inert gas toward the reaction stage on the solid material. Such two-stage process makes easy the control of the temperature of both the vaporization stage and the reaction stage. As shown by the Applicant, both model and industrial real waste plastics may be used in the PTO or PTF process of the invention.

[0021] Another advantage is that the vaporization and reaction temperature can be decoupled which allows one to tune the reaction temperature in order to modulate either liquid or light olefinic products depending to the downstream applications.

[0022] Accordingly, in a first aspect, the present invention provides a use of a metal-free carbon material for converting plastic into C_2-C_4 olefins and/or other hydrocarbons, under direct induction heating at temperature less than or equal to 800°C, preferably less or equal to 700°C and even preferably less or equal to 600°C.

[0023] In a second aspect, the present invention provides a process for converting plastic into C_2-C_4 olefin and/or other hydrocarbons, comprising a reaction step under direct induction heating, with a metal-free carbon material, at temperature less than or equal to 800 °C, preferably less or equal to 700°C and even preferably less or equal to 600°C.

[0024] "Metal-free carbon material" refers herein to a material that is substantially free of metal, or preferably is totally free of metal. "Substantially free" means that the material has a metal concentration which of less than 3000 ppm, or less than 2000 ppm, or less than 1000 ppm. For example, the material may be constituted by at least 80 wt.% of carbon, or preferably at least 95 wt. % of carbon, and especially, at least 99 wt.% of carbon. The elements constituting the non-carbon part of the material may be at least one element selected among Na, K, Si, S, N and O. The use of plain carbon-based materials, without any additives or promoters, is advantageous as it displays stronger resistance towards deactivation through encapsulation by deposit carbon or coke precursors, as encountered with zeolite-based materials, or chemical properties modification in the presence of organic or inorganic impurities in the processed waste polymers. Advantageously, the spent carbon-based material can be regenerated through chemical leaching without appreciable activity loss due to their high chemical inertness compared to other catalysts or materials.

[0025] Advantageously, the metal-free carbon material may have a BET surface area of at least 0.10 m^2/g, such as for example from 0.10 to 2000 m^2/g, or from 0.10 to 1000 m^2/g, or from 0.10 to 100 m^2/g, or from 1.0 to 400 m^2/g, or from 4.0 to 400 m^2/g, or from 0.10 to 5.0 m^2/g, or from 0.5 to 3.0 m^2/g, such as from 1.0 to 5.0 m^2/g, or from 1.0 to 3.0 m^2/g, as determined by ASTM-D-3663 (Standard Test Method for Surface Area of Catalysts and Catalyst Carriers, 2020). Advantageously, there is no technical limitation for a maximum BET value. A very high BET value means the presence of micropores which have no particular function but which do not interfere with the reaction. Advantageously, the carbon material could have a geometric structure allowing a good connectivity between its primary particles, and therefore a high intrinsic thermal conductivity of the carbon material allowing the high heat dissipation within its matrix.

[0026] Several forms of carbon can be applied as a material in the present invention. In some preferred embodiments, said carbon material may be selected from the group comprising or consisting of graphite, graphene, carbon black, acetylene black, pyrolytic carbon, activated carbon and any combinations thereof. Such carbon-based materials could be also produced with different size and shape.

[0027] The term "graphite" as used herein, refers to the crystalline form of the element carbon with its atoms arranged in a hexagonal structure. A graphitic carbon has the characteristics of an ordered three-dimensional graphite crystalline structure consisting of layers of hexagonally arranged carbon atoms stacked parallel to each other as determined by X-ray diffraction. The term graphite herein used includes both natural graphite, i.e. essentially in its geologically occurring natural crystalline form, and synthetic graphite, i.e. synthetically prepared or processed graphite. Examples of natural graphite include so-called amorphous (nanocrystalline) graphite, flake graphite, and vein graphite. Examples of synthetic graphite include pyrolytic graphite, highly oriented pyrolytic graphite (HOPG), synthetic graphite flakes. The term "synthetic graphite" as used herein unless further qualified also intends to include nonexpanded graphite.

[0028] The term "graphene" as used herein, refers to a polycyclic aromatic molecule with carbon atoms covalently bonded to each other in a same plane. The covalently bonded carbon atoms can form a six-member ring as a repeating unit, and may also include at least one of a five-member ring and a seven-member ring. Multiple graphene layers are referred to in the art as graphite. Thus, graphene may be a single layer, or also may comprise a multiple layers of graphene that are stacked on other layers of graphene. Generally, graphene has a maximum thickness of about 100 nanometers (nm), specifically about 5 nm to about 90 nm, more specifically about 20 nm to about 80 nm. Graphene can be also used in the form of expanded graphite where the graphite structure was partially expanded through incorporation of molecules such as HNO_3, KOH between the layers, to generate a graphite-like structure with high accessibility.

[0029] The term "carbon black" as used herein, refers to a form of carbon having a high surface-area-to-volume ratio, albeit lower than that of activated carbon, with a short range ordered structure. Carbon black is a material produced by the incomplete combustion of coal and coal tar, vegetable matter, or petroleum products, including fuel oil, fluid catalytic cracking tar, and ethylene cracking.

[0030] The term "acetylene black" as used herein, refers to a carbon black produced by thermal decomposition of acetylene, having a high purity and few factors for inclusion of impurities among many carbon blacks, a high crystallinity and a developed structure.

[0031] The term "pyrolytic carbon" refers to any form of carbon obtained by pyrolysis of an organic feedstock.

[0032] The term "activated carbon" as used herein, refers to a form of carbon having small, low-volume pores that increase the surface area available for adsorption or chemical reactions. It can be produced from various sources such as bamboo, coconut husk, willow peat, wood, coir, lignite, coal, and petroleum pitch that are pyrolyzed and submitted to a subsequent activation treatment aimed at generating micropores. Carbon activation may be operated by any method known by the skilled person.

[0033] A carbon material as used in the present invention may have different morphologies. The morphology or form of the carbon material is not particularly limited and may for instance include grain, felt, fiber, for example nanofiber, filament, 2D or 3D fabrics, foam as open cell foam, 3D-printed structures, sphere, cloth, monolith, extrudates as honeycombs, rodshaped, sticks and particles, tube, for example nanotube, ring, trilobes, tablets and nanotablets, and any combinations thereof.

[0034] For example, the carbon material may be a graphite felt. The term "graphite felt" (GF) as used herein refers to a textile material that predominantly comprises randomly oriented and intertwined carbon filaments or fibers, that has been subjected to a graphitisation process, which may involve heat treating the carbon felt at high temperatures, such as in the range of about 2600°C to about 3300°C. During the graphitising process, the randomly oriented and intertwined carbon filaments or fibers may be converted into a three-dimensionally ordered graphite structure. A preferred example of a carbon material for use in the present invention is graphite felt, preferably with the following dimensions: fiber diameter of ca. 10 μm and length up to several millimetres.

[0035] Another example of carbon material is carbon felt. The term "carbon felt" (CF) as used herein refers to a textile material that predominantly comprises randomly oriented and intertwined carbon filaments or fibers. Without limitation, carbon felt suitable for use in the instant invention is commercially available e.g. from Avcarb or Cera Materials. Advantageously, the carbon felt may have a thickness of from about 2 mm to about 20 mm. For example, the carbon felt may have a thickness of from about 4 to about 15 mm, from about 6 to about 10 mm, or from about 2 to about 6 mm. The CF can be also used with different configurations, e.g. as such, planar or in "rolled" configuration, for giving a different surface contact and length depending to the downstream applications.

[0036] Another example of carbon material is "carbon nanotube" or "CNT" that may refer to a hollow cylindrical or tube shape carbon structure, defining a void therein, which may be empty or filled with another material. CNTs may be closed at one or both ends. CNTs may be conceptualized as rolled graphene sheets, having a hexagonal lattice of carbon molecules with basal planes exposure. Depending on the rolling degree and the way the original graphene sheet is formed, carbon nanotubes of different diameter and internal geometry can be formed. Carbon nanotubes formed by rolling up of a single sheet forming the aforementioned cylinder, are called "single-walled" carbon nanotubes. The carbon nanotubes formed by rolling up more than one sheet of graphene with a structure that resembles a series of concentric cylinders of increasing diameters from the center to the periphery are called "multi-walled" carbon nanotubes. Suitable carbon nanotubes for use in the present invention encompass single-walled carbon nanotubes as well as multi-walled carbon nanotubes. In certain embodiments wherein carbon nanotubes are multi-walled carbon nanotubes, the multi-walled carbon nanotubes comprise 2 or more, such as from 2 to 20, or 5 to 50, graphitic layers. In certain embodiments, carbon nanotubes as used herein have a high aspect ratio, i.e. length-to-diameter ratio, preferably an aspect ratio of between 10 and 10,000,000 to 1, such as between 100 and 10,000 to 1. In certain embodiments, carbon nanotubes as used herein have an average outer diameter of about 2 to 100 nm, such as about 5 to 50 nm, such as about 8 to 30 nm, such as about 20 nm. The average inner diameter of carbon nanotubes as used herein can be about 0.5 to 100 nm, or about 1 nm to 50 nm.

[0037] Another example of carbon material is "carbon nanofiber" or "CNF" including a carbon-containing material comprising a solid cylindrical shape, with prismatic planes exposure, mostly free of voids meaning without a hollow central portion, despite some small channel could exist. A carbon nanofiber may be similar to a carbon nanotube (CNT), but may include a solid core rather than a hollow central portion, and prismatic planes, with higher reactivity, exposure instead of basal ones. Carbon nanofibers may also be in the form of stacked graphene sheets. Carbon nanofibers may be formed through any method known in the art, including deposition from carbon containing vapour, such as by catalytic chemical vapour deposition (CCVD) wherein carbon is deposited in the presence of a transition metal catalyst on a macroscopic substrate, or other methods of forming carbon nanofibers known in the art.

[0038] Advantageously, carbon nanofibers may have a length of about 100-1000 nm, such as about 150-500 nm. In certain embodiment, carbon nanofibers as used herein may have the aspect ratio, i.e. the ratio of length to the outer diameter, of preferably more than about 10, such as more than about 50, or more than about 100, or more than about 1000, or more than about 2000.

[0039] Advantageously, carbon nanofibers as used herein may have a mean average diameter less than 1000 nm. In certain embodiments, the carbon nanofibers have a mean average diameter less than 500 nm, such as less than 300 nm. For example, carbon nanofibers may have a mean average diameter between about 50 and 300 nm, such as between about 50 and 250 nm.

[0040] It is worthy to note that both CNT and CNF can be grown on macroscopic substrates such as ceramics or oxides, i.e. silicon carbide, silica, alumina, and the combination of them, or also on other host substrates such as activated carbon. Such structured composites could allow one to control the flow pattern within the solid bed as well as to increase the surface contact between the reactant and the solid.

[0041] Other examples of suitable forms of carbon materials include grains having an average particle diameter of 0.1

to 5 mm, extrudates with an average particle diameter of 1 to 5 mm and lengths up to 2, 3, 4, 5, 6 or more mm, trilobes with an average particle diameter ranged between 1 to 5 mm and length between 1 to 10 mm, foams with ppi (pores per inch) ranged from 60 to 5 ppi, honeycombs with cpsi (cells per square inch) ranged from 5 to 900, tubes with aspect ratios of about 5:1 (meaning 1 mm diameter x 5 mm long), 3:1 or 2:1, depending on the diameter of the material.

[0042] As mentioned above, the carbon material may be a combination of at least two materials as defined above.

[0043] Advantageously, the metal-free carbon material may be supported by a non-carbon structure such as alumina, silica, silicon carbide or other oxides or ceramics or the combination of them. As an example, a graphene coating can form a continuous film on the host substrate which confers a high electric connectivity in the carbon material and allow an efficient heating under induction mode. The graphene coating can be also applied on activated carbon structure in order to improve the electrical connectivity. Such connectivity will significantly improve the heat harvesting from the induction coil leading to a temperature increase in the composite. Optionally, such a better connectivity may allow reducing the heating power to be delivered to the carbon material.

[0044] "Plastic" refers herein to any synthetic material made of organic polymers and that can be molded into shape while soft, and then set into a rigid or slightly elastic form. It may be for example at least one selected among high-density polyethylene (HDPE) and low-density polyethylene (LDPE), polypropylene, polystyrene, mixed industrial waste plastic, as low-density polyethylene, PET, PVC and polystyrene containing solid residue and plastics containing solid residue.

[0045] "C_2-C_4 olefins" refers herein to at least one aliphatic alkenes chosen among ethylene, propylene and butylene. Preferably, it may be ethylene and/or propylene. According to the invention, the plastic may be converted into one specific olefin, or into a mixture of olefins. In some cases, the conversion may not be complete, and possible traces of diolefins may occur, such as diolefins made from ethylene, propylene and butylene.

[0046] "Other hydrocarbons" refers herein to any hydrocarbons that are not C_2-C_4 olefins. It may be for example liquid hydrocarbons having at least 5 carbon atoms, for example fuel, and/or paraffinic gaseous C_1 to C_4 hydrocarbons. It may refer to a mixture of at least two of these hydrocarbons.

[0047] "Direct induction heating" refers herein to a process wherein the carbon material is directly heated by a current, generated on the surface of the carbon material through interaction with an electromagnetic field provided by an inductor. In an embodiment of the invention, the carbon material may be heated by generating an alternating electromagnetic field within a reaction zone containing said carbon material, where the alternating electromagnetic field passes through the reaction zone thereby generating an electric current in said carbon material and heating the carbon material. Advantageously, the high intrinsic thermal conductivity of the carbon material allows a rapid heat transfer from the outer surface to the core of the material.

[0048] Advantageously, the step of direct induction heating may be carried out at a reaction pressure comprised between 0.5 and 20.0 bar, for example between 1 and 5.0 bar.

[0049] Advantageously, the use of the invention may be carried out in a two-stage process. Indeed, in the process of the invention, the plastic may be vaporized, without any presence of catalyst or in the presence of some materials which can harvest the heat from the oven in order to improve the heat transfer to the plastic, in a first step, while vapors are swept toward the material in a second step, where a cracking step under direct induction heating takes place.

[0050] The vaporization step advantageously allows the vaporization of the plastic waste. It may be realized by any method commonly used by the skilled person in order to vaporize the plastic waste, for example Joule heating, or microwave heating thanks to SiC or carbon particles mixed with the raw plastic. The vaporization conditions may be determined by the skilled person, depending on the kind and amount of plastic waste. It may be for example a temperature comprised between 300°C and 600°C, advantageously about 500°C and preferentially about 450°C. For example, the vaporization step may be realized in a first-stage reactor. Then, the plastic vapors may be swept, for example with an inert gas such as argon or nitrogen, toward the solid material in a second-stage reactor, where the cracking process takes place. The C_2-C_4 olefins and/or other hydrocarbons are then obtained. In another operation mode other gas such as hydrogen or other light hydrocarbons can also be used.

[0051] The process can be operated in continuous mode and therefore the operating time of the different steps depends on the amount of plastic to be processed.

[0052] Depending on the carbon nature, i.e. non-porous vs porous, the liquid vs gaseous fraction can be tuned by changing the reaction conditions. For example, on non-porous material under the reaction conditions as exemplified in the examples gaseous fraction could be produced as the main fraction, with mostly light olefins as the main product, while on porous material the liquid fraction is higher with respect to the gaseous one, with liquid fraction from C_6 to C_{25} depending to the reaction temperature.

[0053] Advantageously, the resulting liquid hydrocarbons (also named "liquid fraction") may be condensed, and/or the gaseous resulting products (also named "gas fraction") may be directed to gas chromatography for analysis. Advantageously, the gas fraction may comprise at least 5.0 mol% of unsaturated C_2 to C_4 hydrocarbons, and preferably at least 25.0 mol% or preferably at least 40.0 mol% or preferably at least 45.0 mol% of unsaturated C_2 to C_4 hydrocarbons.

[0054] Advantageously, liquid fraction, generated on porous carbon material, can be used as such in different chemical processes, i.e. fuel for transportation, or it could also be recycled onto the carbon material for being cracked down into light olefins, i.e. C_2-C_4 olefins.

[0055] This invention is further illustrated by the following examples with regard to the annexed drawings that should not be construed as limiting.

Brief description of the figures

[0056]

- Figure 1: represents Plastic-to-Olefins (PTO) process (selectivity wt.%) on planar Carbon Felt (CF) material as a function of the reaction temperature under direct induction heating for converting model HDPE. (A-B) Gaseous and liquid products distribution (H_2 and C_n), (C-D) Gaseous products distribution (H_2 and C_1-C_7). Reaction conditions: HDPE weight = 6 g (mixed with 2 g of SiC for improving the heat transfer), CF weight = 0.54 g, reactor diameter = 26 mm, argon flow rate = 15 mL. min^{-1}, HDPE vaporization temperature = 450 °C, CF temperature = variable.
- Figure 2: represents Plastic-to-Olefins (PTO) process (selectivity wt.%) on planar Carbon Felt (CF) material as a function of the reaction temperature under indirect Joule heating for converting model HDPE. (A, B) Liquid and gaseous products distribution (H_2 and C_n including almost solid waxes), (C, D) Gaseous products distribution (H_2 and C_1-C_7). Reaction conditions: HDPE weight = 6 g (mixed with 2 g of SiC for improving the heat transfer), CF weight = 0.54 g, reactor diameter = 26 mm, argon flow rate = 15 mL. min^{-1}, HDPE vaporization temperature = 450 °C (heating rate of 20 °C. min^{-1}), CF temperature = variable.
- Figure 3: represents Plastic-to-Olefins (PTO) process (selectivity wt.%) on rolled CF material for converting model HDPE: (A, C, E) as a function of the reaction temperature and (B, D, F) C_2-C_4 olefins vs saturated fraction for gaseous products ranged from C_1 to C_7 under direct induction heating. Reaction conditions: HDPE weight = 6 g (mixed with 2 g of SiC for improving the heat transfer), rolled CF weight = 1.2 g, reactor diameter = 26 mm, argon flow rate = 15 mL. min^{-1}, HDPE vaporization temperature = 450 °C (heating rate of 20 °C. min^{-1}), CF temperature = variable.
- Figure 4: represents Plastic-to-Olefins (PTO) process (selectivity wt.%) on CF materials, i.e. planar and rolled, operated under IH mode at 550 °C for planar CF and 500 °C for rolled CF for converting model HDPE plastic into light olefins. (A, C) Product distribution. (B, D) Olefins vs gaseous saturated C_2-C_4 fraction. Reaction conditions: HDPE weight = 6 g (mixed with 2 g of SiC for improving the heat transfer), CF weight = 0.54 g (planer CF) and 1.2 g (rolled CF), reactor diameter = 26 mm, argon flow rate = 15 mL. min^{-1}, HDPE vaporization temperature = 450 °C (heating rate of 20 °C. min^{-1}).
- Figure 5 represents Plastic-to-Olefins (PTO) process (selectivity wt.%) using a mixed industrial polymer waste on CF materials, i.e. planar and rolled CF, operated under IH mode at 550 °C for planar CF and 500°C pour rolled CF, for converting industrial mixed waste plastics into light olefins. (A, C) Product distribution and C_2-C_4 fraction on rolled CF material, (B, D) Product distribution and C_2-C_4 fraction on planar CF material. Reaction conditions: mixed industrial plastic weight = 6 g (mixed with 2 g of SiC for improving the heat transfer), CF weight = 0.54 g (planar CF) and 1.2 g (rolled CF), reactor diameter = 26 mm, argon flow rate = 15 mL. min^{-1}, HDPE vaporization temperature = 450 °C (heating rate of 20 °C. min^{-1}).
- Figure 6 represents the cycling tests of the plastic-to-Olefins (PTO) process on rolled CF material (diameter, 26 mm, height, 15 mm) at 450 °C operated under IH mode for converting industrial mixed waste plastics into light olefins. (A-C) Product distribution as a function of the cycling tests. (D-F) Olefins vs saturated C_2-C_4 fraction as a function of the cycling tests (Cycle 1, cycle 3 and cycle 9). Reaction conditions: HDPE weight = 6 g (mixed with 2 g of SiC for improving the heat transfer), CF weight = 1.2 g (rolled CF), reactor diameter = 26 mm, argon flow rate = 15 mL. min$^{-\backslash 1}$ or 30 mL. min^{-1}, HDPE vaporization temperature = 450 °C (heating rate of 20 °C. min^{-1}).
- Figure 7 represents (A) Gas and liquid fraction distribution and (B) olefins C_2-C_4 fraction as a function of cycling tests during the PTO process on rolled CF material (diameter, 26 mm, height, 15 mm) at 450 °C operated under IH mode for converting industrial mixed waste plastics into light olefins. Reaction conditions: Mixed waste plastic weight = 6 g (mixed with 2 g of SiC for improving the heat transfer) was used for each cycle, CF weight = 1.2 g (rolled CF), reactor diameter = 26 mm, argon flow rate = 30 mL. min^{-1}, vaporization temperature = 450 °C.
- Figure 8 represents Plastic-to-Fuels (PTF) process (selectivity wt.%) using model HDPE polymer on 3mm pellets of MESOC+ material under direct induction heating (500 °C) and indirect Joule heating mode (500 and 550 °C). (A, B) Liquid and gaseous products distribution (H_2 and C_n) and gaseous products distribution (H_2 and C_1-C_7) under direct induction heating. (C-F) Liquid and gaseous products distribution (H_2 and C_n including also solid waxes) and gaseous products distribution (H_2 and C_1-C_7) under indirect Joule heating. Reaction conditions: HDPE weight = 6 g (mixed with 2 g of SiC for improving the heat transfer), MESOC+ weight = 3 g, reactor diameter = 26 mm, argon flow rate = 15 mL. min^{-1}, HDPE vaporization temperature = 450 °C (heating rate of 20 °C. min^{-1}).
- Figure 9 represents Plastic-to-Fuels (PTF) process (selectivity wt.%) on (A, B) 3mm pellets of MESOC+ and (C, D)

1mm pellets of MESOC+ material at 500 °C under induction heating. Reaction conditions: HDPE weight = 6 g (mixed with 2 g of SiC for improving the heat transfer), MESOC+ weight = 3 g, reactor diameter = 26 mm, argon flow rate = 15 mL. min^{-1}, HDPE vaporization temperature = 450 °C (heating rate of 20 °C. min^{-1}).

- Figure 10 represents Plastic-to-Fuels (PTF) process (selectivity wt.%) using model HDPE polymer (A, B) and mixed industrial polymers (C, D) on 3mm pellets of MESOC+ material under direct induction heating. Reaction conditions: HDPE weight = 6 g (mixed with 2 g of SiC for improving the heat transfer), MESOC+ weight = 3 g, reactor diameter = 26 mm, argon flow rate = 15 mL. min^{-1}, HDPE vaporization temperature = 450 °C (heating rate of 20 °C. min^{-1}), MESOC+ temperature = 500 °C.
- Figure 11 represents Cycling tests for the Plastic-to-Fuels (PTF) process (selectivity wt.%) on 3mm pellets of MESOC+ material operated under IH mode at 500 °C for converting model HDPE into fuels. (A, C, E) Product distribution as a function of the number of cycles (A-B: cycle 1, C-D: cycle 2 and E-F: cycle 3. (B, D, F) Olefins vs saturated C_2-C_4 fraction as a function of the number of cycles. Reaction conditions: HDPE weight = 6 g (mixed with 2 g of SiC for improving the heat transfer), MESOC+ weight = 3 g, reactor diameter = 26 mm, argon flow rate = 15 mL. min^{-1}, HDPE vaporization temperature = 450 °C (heating rate of 20 °C. min^{-1}).

Examples

Example 1: material for carrying out the process of the invention

[0057] A device for carrying out the invention comprises a first section, which is a polymer supplier which can contain a polymer weight from about 5 to 100 g. The reservoir of this polymer supply section was continuously flushed with an argon flow (30 mL. min^{-1}) in order to avoid any air infiltration inside the reservoir. The polymer extrudates were feed to a vaporization stage localized within an electric furnace (Joule heating) kept at 450 °C and continuously flushed with an argon flow with various flow rate ranged from 15 to 60 mL. min-’. The polymer vapors generated at this stage were brought to the reaction section (also named "cracking stage") operated either under direct contactless induction heating "IH") or indirect Joule heating ("JH") at different temperatures. The reaction products were further passed through a trap maintained at 16 °C for condensing the liquid hydrocarbons while the gaseous products were directed to the gas chromatography (GC) for analysis. The reaction products were analyzed on-line by two VARIAN 3800 gas chromatographs. The first one equipped with two detectors (thermal conductivity detector (TCD) connected to an Agilent J&W DB-1 column and a flame ionization detector (FID) connected to an Agilent J&W CarboBOND column) was used to analyze H_2/CH_4 and hydrocarbons up to C_{12}, respectively. The second one equipped with a FID detector connected to a Restek RT alumina BOND column, was employed to separate lighter hydrocarbons such C_2H_2, C_2H_4 and C_2H_6 and other hydrocarbons up to C_7. Calibration curves were used to quantify CH_4, H_2, C_2 fractions, C_6H_6, C_7H_8, C_8H_{10}, and $C_{10}H_8$. The Dietz factor method was used for the calculation of other hydrocarbons using the areas of FID integration.

[0058] The IH experiment was conducted on an EasyHeat® 8310 induction heating setup (10 kW, Ambrell Ltd) equipped with a spiral 6-turn induction coil (L = 1.05 m, pure coil resistance = 2.066×10^{-3} Ω) and external cooling chiller with recirculated water/glycerol (10%) mixture as cooling media. In a typical experiment, one quartz reactor containing the material, similar to that used for the JH, was placed inside the induction heater coils. The realtime temperature control/regulation was ensured by a PID system (Proportional Integral Derivative controller, Eurotherm model 3504) connected to a laser pyrometer (Optris®, power < 1 mW, located at ≈ 30 cm from the material) focused on the middle of material bed and with the capability of working in 150 - 1000 °C range. The heating/cooling rate allowed for the system is about 300 °C min^{-1} in the 160 - 300 °C temperature range. It is worthy to note that the inductor operated at a frequency of 263 kHz, which generated a much lower magnetic field compared to those operated at lower frequency, i.e., < 10 kHz. Indeed, magnetic fields from low frequency induction are more penetrating to the surrounding material. However, in order to further reduce the exposure of the worker to the magnetic field, the setup was localized inside a Faraday cage surrounded with metal mesh.

[0059] For indirect Joule heating, the material was localized within an electric oven set at the reaction temperature and controlled by a thermocouple inserted inside the ceramic section of the oven.

[0060] For the PTO and PTF processes, both model waste plastics, i.e. high-density polyethylene (HDPE), and mixed industrial waste plastic, i.e. low- and high-density polyethylene (LDPE) and polystyrene (PS) containing solid residue, were investigated.

[0061] Two kinds of carbon materials are used in the present work: (i) low specific surface area, 4 m^2/g, non-porous carbon felt (commercialized by MERSEN Com.) constituted by entangled carbon microfilaments with an average diameter of ca. 10 μm and length up to several hundred micrometers and (ii) porous carbon (MESOC+, commercialized by SICAT SARL) produced industrially with a specific surface area of 300 m^2/g and constituted with a large mesoporous network. The different characteristics of these carbon-based materials are presented in Tables 1 to 3.

Table 1: Characteristics of the different carbon materials used in the process.

Material	Specific surface area (m^2/g)	Producer	Appearance
Carbon felt	4	MERSEN Com.	Purchased in a form of carpet macroscopic shape with dimension of 1.5 m (width) and 2.0 m (length) with a thickness of 12 mm
MESOC+	297	SICAT SARL	Extrudates shape with diameters of either 1mm or 3mm, 2 to 4mm in length

[0062] The detail characteristics of the carbon felt according to the purchaser are summarized in Table 2.

Table 2: Properties of pristine carbon felt (information provided by the supplier).

Property	Value
Density at 20°C	0.08 g/mL
Carbon content	99.5 %
Ash	500 ppm
Specific Heat	0.71 J/g/° C
Mean Specific Heat	1.67 J/g/° C
Emissivity	0.99
Sublimation Temperature	3600
Surface Area (Nitrogen)	4 ± 3 m^2/g
Thermal Conductivity	-
Approx. Processing Temperature	2500 °C

[0063] The detail characteristics of the MESOC+ according to the purchaser are summarized in Table 3.

Table 3: Typical properties of fresh MESOC+ (information provided by the supplier for 3mm pellets).

Property	Value
Crushing strength (ASTM D4179)	40 N/mm
Attrition (ASTM D4058)	<1%
Tapped bed density	580 g/L
BET surface area	300 m^2/g
Pore volume for pore diameters between 6 and 100nm (Hg intrusion)	0.48 mL/g

Example 2: Polymer cracking process

PTO on Non-Porous Carbon Felt Material

[0064] The carbon felt (CF) purchased from Mersen Co. was used without any pretreatment. The CF is constituted by entangled microfilaments with an average diameter of ca. 10 μm and length up to several hundred micrometers. The CF microfilaments are very smooth and contain almost no internal porosity and roughness, which is in good agreement with their low specific surface area. The material also displays a high open voidage up to about 90 vol. %.

[0065] For being used as metal-free material, the CF can be directly cut into planar disk or in sheet shape, noted planar CF, which can be further rolled up to produce a cylindrical shape, noted rolled CF. The rolled CF material seems to be the best configuration for being used as carbon material for the waste plastic conversion process as its length can be easily tuned, which allows one to adapt the bed height to control the contact time and exposure surface with respect to the plastic vapors which could improve the light olefins yield. Indeed, such control of bed height is not as efficient in the case of planar CF configuration, because stacking several planar CF pieces one on another results in an inhomogeneous heating of the solid bed. Indeed, the loose contact between two successive CF pieces could induce local overheating resulting to an inhomogeneous temperature distribution within the solid bed and excessive decomposition of the intermediate compounds into carbon. Recent studies on catalytic systems under microwave heating (MW) have indicated that at the contact points between two silicon carbide spheres the temperature could present a maximum difference of up to 240°C (Haneishi et al., 2019 ([10])). It would seem after these studies that this value represents the maximum difference in temperature recorded in a catalytic reactor heated under microwaves.

[0066] Another advantage relies on the use of plain carbon materials, without any additives or promoters, which display stronger resistance towards deactivation through encapsulation by deposit carbon or coke precursors, as encountered with zeolite-based materials, or chemical properties modification in the presence of organic or inorganic impurities in the processed waste polymers. The spent carbon materials can be regenerated through chemical leaching without appreciable activity loss due to their high chemical inertness compared to the other materials or catalysts. The macroscopic structure of the CF is produced through a technique called needle punching to generate oriented interwoven structure inside the CF matrix (Xie et al., 2020 ([11])). According to the needle punching process the planar CF displays a higher preferential path, i.e. needle mark holes, compared to the rolled one. For the tests, two configurations of CF materials are evaluated: planar and rolled one.

PTO Process on Model HDPE Plastic Waste

[0067] In this example, the conversion of model waste plastic (HDPE) into light olefins is carried out on CF material under both direct induction heating and indirect radiative Joule heating. The results obtained, as a function of the reaction temperature, are presented in Figures 1 to 4.

[0068] The cracking performance on the planar CF material operated under IH mode increases from 500 °C to 550 °C, i.e. gas fraction increases from 53 % to 76 % (Fig. 1A-B). Liquid fraction is mostly composed of long-chain hydrocarbons ranged between C_{19} to C_{30} with a small fraction of C_{30} to C_{35} as show in Fig. 1A-B. The small fraction of long-chain hydrocarbons could be attributed to the high void fraction of the CF material, i.e. 90 % of empty volume, which could favor some by-pass of the polymer vapors during the test. Blank test carried out under Joule heating with quartz wool instead of CF only yields long-chain hydrocarbons (C > 30) which cannot be dissolved in any solvent and no trace of hydrocarbons with carbon chain smaller than 30 can be observed.

[0069] The C_2-C_4 olefins vs saturated gaseous fraction obtained as a function of the reaction temperature on the planar CF material under IH also shows the same trend with a C_2-C_4 olefins yield of 33 % at 500°C and 51 % at 550 °C (Figure 1C-D).

[0070] It is worthy to note that the color of the as-produced liquid hydrocarbons also changes as a function of the reaction temperature, i.e. darker as increasing the reaction temperature. Such color change could be attributed to the presence of polyolefins or aromatics in the product. It is expected that such products could be favored at high reaction temperature.

[0071] The PTO process as a function of the reaction temperature was also carried out on the CF material operated under indirect Joule heating and the results are presented in Figure 2. At 500 °C, only waxes are obtained on the CF material and the results are not reported as such waxes can hardly be dissolved in a solvent for GC analysis. The products distribution is radically different under JH mode as at reaction temperature of 550 °C and 600 °C, gas fraction constitutes only to 23 and 39 wt.%, respectively (Figures 2A and B). Inside the gas fraction C_2-C_4 olefins are predominant. Their absolute wt.% is 12 and 22 wt. % based on the initial weight of the waste plastic, respectively at 550°C and 600°C. The liquid fraction recovered at the reactor outlet is mostly constituted by waxes which cannot be dissolved as shown the digital photos presented in inset of Figures 2A and B.

[0072] Such results clearly confirm the high efficiency of the direct IH mode to operate carbon material for the PTO process at low reaction temperature. The high PTO efficiency observed on the CF material under IH could be attributed to several facts: (i) high temperature maintaining efficiency due to the high heating rate of the IH, i.e. several hundred degrees per minute for temperature adjustment, in order to maintain the material temperature for the endothermic cracking reaction; and, (ii) better temperature homogeneity within the entire solid bed as the heat is generated directly within the material body and not through convection/conduction indirect transfer as encountered with the indirect Joule heating mode. Indeed, carbon felt is well known as insulator shield material to prevent heat transfer for high temperature oven, and thus, the carbon filaments display high heat transfer along its filamentous structure but not between the filaments due to the presence of large voidage in the material. In the case of IH, the entire solid volume can be heated while in the case of JH the heat is transferred along the external filaments to the core of the solid bed which is more affected by the filamentous structure of the material. Such heat resistance can be avoided with IH as heat is directly generated through the material body as discussed above and the heat distribution throughout the carbon microfilament is much faster due to the small diameter of the microfilaments which remains within the range of depth penetration for the eddy currents, i.e. few micrometers from the outer surface. The high aspect ratio (length vs diameter) of the carbon microfilaments constituting the CF material also contributes to rapid heat conduction along the filaments and through the entire material matrix and thus, greatly improve the reaction process. By comparing the results between Figures 1 and 2, one can definitively prove the advantages of operating the PTO process with a direct and contactless induction heating mode.

Influence of the CF macroscopic shape

[0073] In another attempt, a rolled CF material was used instead of planar one and the results are presented in Figure 3 as a function of the reaction temperature. At reaction temperature of 500°C, the main fraction of the starting plastic is converted into light hydrocarbons (Figures 3C and 3D), which is not the case for lower reaction temperature, i.e. 450°C (Figures 3A and 3B), where some liquid fraction is observed. At 500°C, the C2-C4 olefins fraction contributes for 46% of the total hydrocarbon products (Figure 3D), this fraction being mainly composed of ethylene and propylene, while methane contributes to ca. 13 wt.%. Increasing the reaction temperature from 500°C to 550°C leads to a sharp increase of the cracking products with a significant contribution of methane, i.e. 29 wt.% (Figure 3F) along with a significant decrease of light olefins. It is expected that at higher reaction temperature, i.e. 600°C, the light olefins are over cracked to yield methane and also some hydrogen. Ethylene remains the main light olefin with a contribution of ca. 22 wt.% (Figure 3F). The results obtained indicate that the rolled CF displays higher cracking performances compared to its planar counterpart (with the same apparent volume) at the same reaction temperature. Such results could be attributed to the orientation of the CF within the induction coil, i.e. circular rolling, which could favor the circulation of the eddy currents from the induction heater within the piece of CF leading to a higher heat harvesting and temperature homogenization within the solid bed.

[0074] The PTO results obtained on the planar and rolled CF materials are compared in Figure 4. According to the results, the CF rolled displays higher PTO performances compared to the planar one as the same cracking and production of C_2-C_4 olefins are obtained on the rolled CF material at lower reaction temperature than the one on the planar CF one, i.e. 500 °C vs 550 °C (Figures 4B and D). The amount of higher hydrocarbons, i.e. > C_{25}, is also significantly lower on the rolled CF material, which confirms the high efficiency of the rolled CF material to crack down the long-chain polymers passing through it even at lower temperature (Figure 4A and C). Such results could be attributed to the difference in terms of carbon microfilaments density between the two structures. Indeed, in the case of CF, produced by a needle punching process, one should have expected to have higher by-pass channels in the planar structure material compared to the rolled one where side face was exposed. The circular orientation of the rolled CF material also favors the induction current which improves the axial heat transfer.

PTO Process on Industrial Plastic Waste

[0075] In this example, the PTO process was investigated on CF materials, i.e. planar and rolled, using a mixture of plastic wastes from different industrial sources (Table 4). The waste plastic was heat treated at 250 °C under argon, in order to melt down the polymers and to measure the exact amount of inorganic solid in the sample.

[0076] Table 4: Composition of the mixed industrial polymer waste and the origin of the waste. The PE contributes to > 50 wt.% and PS < 20 wt.% while the other components are non-plastic solid wastes.

Product names	Description	Preliminary use	Appearance	Weight (%)
LD Polyethylene	Plastic film	Agriculture pallet wrap	White/Clear/Col ored film	> 50
LLD Polyethylene	Colored plastic film	Industrial film wrap	Green/Black/Wh ite film	
HD Polyethylene	Plastic bottles - drums	Soft drink, milk, containers	White/Clear/Col ored materials	
Polystyrene	Packaging material	Agriculture boxes, electronic packaging	White/Colored material	< 20
Non-plastic solid waste		Industries	Brown dark particles	< 30

[0077] The results show that the CF material, regardless the shape and configuration, operated under IH mode displays high cracking performance to convert mixed industrial polymers into liquid and gaseous hydrocarbons (Figures 5A and B). Both materials also display high selectivity towards C_2-C_4 olefins at reaction temperature as low as 500°C (Figures

5C and D). The C2-C4 olefins fraction amounted to about 43 % on the rolled CF material at 500°C, while it was about 49 % on the planar CF material at 550°C. In both cases, ethylene and propylene are the major products of this C2-C4 olefins fraction. The very similar results obtained on both CF materials when operating the PTO process with industrial mixed polymer could be attributed to the lower density of this later compared to that of the model polymer, i.e. mixture of LDHP and HDPE instead of pure HDPE, which is easy to be cracked.

[0078] The results obtained in the different tests, including model HDPE and mixed industrial waste plastic, are summarized in Table 5 and compared with those reported in the literature.

Table 5:

Material	Feed	Reactor	T (°C)	ΣC_2-C_4 olefins (wt.%)	Ref.
Planar CF	HDPE	Fixed bed / IH	500	33	This work (Fig. 1)
	HDPE	Fixed bed / IH	550	51	This work (Fig. 1)
Planar CF	HDPE	Fixed bed / JH	550	12	This work (Fig. 2)
Planar CF	HDPE	Fixed bed / JH	600	22	This work (Fig. 2)
Planar CF	LDPE (> 50 wt.%), PS (< 20 wt.%), solid residue (20 wt. %)	Fixed bed / IH	550	48	This work (Fig. 5)
Rolled CF	HDPE	Fixed bed / IH	450	31	This work (Fig. 3)
	HDPE	Fixed bed / IH	500	46	This work (Fig. 3)
	HDPE	Fixed bed / IH	550	23	This work (Fig. 3)
Rolled CF	LDPE (> 50 wt.%), PS (< 20 wt.%), solid residue (20 wt. %)	Fixed bed / IH	500	43	This work (Fig. 5)
Fresh FCC	HDPE	Fluid bed	450	22	Ali et al., 2002 ([12])
E-Cat	LDPE in toluene	Riser simulator	500	24	De La Puente et al., 2002 ([13])
E-Cat	Mixed polymers	Fluid bed	460	24	Lin et al., 2007 ([14])
Steamed FCC	HDPE	Spouted bed	475	7	Olazar et al., 2009 ([145)
E-Cat + 50 wt.% of bentonine	HDPE	Spouted bed	500	23	Elordi et al., 2012 ([16])
E-Cat	LDPE	Micropyrolyzer	600	45	Eschenbacher et al., 2022 ([16])

Stability as a Function of Cycling Tests

[0079] The stability of the CF materials for converting a mixed industrial waste into light olefins was investigated and the results are presented in Figure 6. The cycling tests are carried out at 450 °C on the rolled CF material, as according to our previous results, this temperature is the most appropriate for performing the PTO process on such material.

[0080] According to the results, the rolled CF material displays a high and stable PTO activity as a function of cycling tests using mixed industrial polymers. Such high stability could be attributed to the following facts: the process was carried out in two-stage, in which the waste polymer was vaporized first in an upper thermal bed, followed by cracking of the polymer vapors in a second reactor containing CF material. The polymer vapors passed through a quartz wool plug, which plays the role of scavenger or filter to block the impurities from the polymer waste and to prevent excessive carbon material deactivation. By operating in such separate sections, the main impurities contained in the raw waste plastics remain in the first thermal bed while much lower impurities, mostly in the gaseous form, passed over the reaction bed which could contribute to its stability as a function of cycling tests. In addition, a layer of 1mm MESOC+ extrudates (2 mm in length) is added on the top of the rolled CF material, slightly out of the induction coil with a temperature of ca. 450°C, in order to play the role of a scavenger layer and also to better vaporize the adsorbed polymer vapors. It is worthy to mention that at this temperature, i.e. 450°C, the MESOC+ sample displays a very low activity without any ability to produce light olefins. The gas, liquid and solid residue fraction obtained after each cycle at 450 °C is presented in Figure 7 and confirms the high stability of the rolled CF material for the PTO process.

[0081] The weight of deposited solid residue as a function of the cycling tests is also measured. According to the results, the carbon material weight slightly increases, by ca 0.6 ± 0.3 wt.% after each cycle, for the first five cycling tests at 500 °C.

PTF on Porous Carbon Materials

[0082] The porous carbon, noted MESOC+, is produced at industrial scale by Sicat SARL (www.sicatcatalyst.com) in the form of extrudates with different macroscopic shapes. For the PTF process, the MESOC+ extrudates with either 1 or 3 mm in diameter and 2 to 4 mm in length were used. Low resolution SEM micrograph carried out on the MESOC+ evidences the roughness of its surface taken under different angles. Medium resolution SEM micrographs evidence the presence of macropores within the material and a highly mesoporous structure which could favor the adsorption and cracking of the pyrolysis polymer vapors.

PTF Process on Model HDPE Plastic Waste

[0083] In this section, the conversion of model waste plastic (HDPE) into HC is carried out on MESOC+ material under both direct induction heating and indirect radiative Joule heating. The results obtained are presented in Figure 8. The 3mm MESOC+ displays a lower cracking activity than the CF materials, i.e. planar or rolled, at the same reaction temperature of 500°C. However, it is worthy to note that the performances obtained on the 3mm MESOC under IH remains much higher than under JH mode even at higher temperature (Figures 8A vs 8C and E). Such results could be again explained by a higher heat maintaining within the carbon bed. Polymer long-chain cracking is an endothermic process and thus, the efficiency of the solid material is strongly influenced by the effective temperature distribution within the bed and on the carbon surface where the reaction takes place. At high cracking rate the material temperature could be lowered and may thus reduce the cracking performance which is at the origin of the formation of long-chain hydrocarbons or waxes. The low heat supply using indirect heating mode cannot allow one to maintain the optimal bed temperature unlikely to induction heating as the heat is generated directly within the material body.

[0084] However, it is worthy to note that the 3mm MESOC+ material mostly yields saturated fraction and also liquid hydrocarbons in the range of C_6 to C_{20} (Figure 9A). Such results are different than those obtained on the non-porous CF material operated under similar reaction conditions where light olefins (C_2=-C_4=) were predominant. Such results could be explained by the following facts: (i) unlike the non-porous CF the porous nature of the MESOC+ could favor diffusion of the pristine light olefins inside the material porosity and thus, favoring the formation of long-chain olefins or aromatics through recombination of light olefins, (ii) the 3mm MESOC+ also displays a higher diffusion length compared to the CF one, i.e. 3 mm in diameter vs 10 μm, which could induce internal temperature gradient inside the extrudates with lower cracking performance. Such hypothesis was investigated by changing the 3mm MESOC (diameter of 3 mm) by a 1mm MESOC+ (diameter of 1 mm). The comparative results are presented in Figure 9. According to the results the smaller carbon material, i.e. 1mm MESOC+, displays improved selectivity in light olefins, despite some liquid hydrocarbons in the range of C_6 to C_{15} are still observed. On the 3mm MESOC+ the long-chain hydrocarbons are up to > C_{23}, while on the 1mm MESOC+ only hydrocarbons containing up to C_{15} are observed. Such results could be explained by the fact that for the 3mm MESOC+ material the heat is transferred from the external surface to the inner part of the pellets, as induction heating of electrical conductive materials mostly starts on the outer surface (skin effect) and the temperature is then transferred inside the material body through conduction. Consequently, the solid temperature is expected to be more homogeneous for 1mm pellets than for 3mm pellets, resulting in an increased cracking activity of the polymer vapors. The small diameter of the 1mm MESOC also improves the geometric contact surface between the polymer vapors and the hot material external surface which increases the cracking performance. However, it is worthy to note that the MESOC+ materials still display lower C_2-C_4 olefins yield compared to the CF ones. Such results could be explained by the porosity present in the MESOC+ materials which could favor secondary reaction, i.e. aromatization, whereas the lack of porosity in the CF material prevents such secondary reaction. However, it is worthy to mention that liquid hydrocarbons produced from the pyrolysis of waste plastics could represent also an interesting option as such products could be converted into different fuel fractions, i.e. gasoline, diesel and jet fuel, with low sulfur content.

PTF Process on Industrial Plastic Waste

[0085] Plastic cracking was also investigated on a MESOC+ material using a mixed plastic waste from different industrial sources (Table 4). The results (Figure 10) show that the 3 mm MESOC+ material operated under IH mode displays high cracking performance and also high selectivity towards light olefins formation at relatively low reaction temperature from the industrial mixed plastic wastes (Fig. 11C and D). The formation of small fraction of long-chain liquid fraction could be attributed to the low vaporization temperature of the mixed polymers that contain LDPE, which could provide a larger amount of polymer vapors at the same pyrolysis temperature compared to that of the model HDPE.

Stability as a Function of Cycling Tests

[0086] The stability of the 3mm MESOC+ material for converting a model HDPE into light olefins and fuel was investigated and the results are presented in Figure 11. The 3mm MESOC+ displays an intermediate behavior with a gas fraction of ca. 55 % and a liquid fraction amounted to about 42 % for all the cycling tests. However, one can notice that for the Cycle#3 a slight increase of the long-chain hydrocarbons, i.e. > C_{17}, can be observed which could be attributed to a partial plugging or encapsulation of some active sites at the origin of the cracking process (Fig. 11E). According to the results, the 3mm MESOC+ material is able to convert waste plastic into liquid and gaseous hydrocarbons for downstream applications such as polymer processing (ethylene and propylene fraction) or liquid feedstock for transportation or petrochemical processing. The C_2-C_4 fraction decreases from Cycle#1 to Cycle#2, from 38 % to 28 %, and remains unchanged at Cycle#3, while C2-C4 olefins fraction increases from 15% to 17% and 20% for cycle 1, cycle 2 and cycle 3. The results obtained again confirm the ability of the MESOC+ material for converting waste plastics into hydrocarbons which could be used in numerous petrochemical processes.

Conclusion

[0087] In summary we have reported the efficient combined use of metal-free carbon materials and direct induction heating for converting waste plastics, either model or industrial mixed, into C_2-C_4 light olefins fraction, especially on non-porous CF material, and liquid hydrocarbons, especially on porous MESOC+ materials. The results have shown that carbon material, either non-porous such as carbon felt or porous ones, are efficient for performing such direct conversion at relatively low temperature under induction heating mode. The carbon materials also display a high stability as a function of cycling tests which again confirms their interest for such process. In this conversion process, the carbon materials are directly heated by the eddy currents, generated on the surface of the material through interaction with the electromagnetic field provided by the inductor. The high intrinsic thermal conductivity of the carbon-based materials significantly improves the heat transfer from the outer surface to the core of the material. It is expected that the heat transfer is more efficient in the case of carbon felt due to the relatively small diameter of the carbon microfilamentous, i.e. 10 μm, which remains within the range of depth penetration for the eddy currents, compared to the mesoporous ones with larger diameter, $\geq$ 1 mm. Such high heat transfers in the carbon felt could be advanced to explain the higher light olefins production from the plastic waste compared to that observed on the larger size mesoporous carbon where temperature gradient within the pellets could hinder the cracking reaction leading to the formation of higher amount of liquid fraction under the same reaction conditions. The difference in terms of light olefins yield between the CF and MESOC+ materials could also be due to diffusion phenomenon between the two materials due to their pore and geometric structure. Induction heating also provides an elegant way to heat up directly the material without excessive energy lost through convection and conduction as usually observed in the case of indirect Joule heating. The results also suggest that carbon materials with smaller dimension, i.e. carbon nanotubes or nanofibers decorated macroscopic host substrates, could be also efficiently heated up using induction heating for performing the PTO or PTF processes.

[0088] The non-porous carbon felt, CF, displays a high selectivity towards C_2-C_4 olefins fraction with essentially ethylene and propylene fraction, at reaction temperature ranged between 450 to 550 °C for both model waste plastic (HDPE) and mixed industrial waste plastic containing impurities. The C_2-C_4 olefins can be finely tuned by modifying the operation parameters such as temperature or contact time. The material also displays a high stability as a function of cycling tests with industrial mixed waste plastic which highlight the advantages of using such metal-free carbon materials. Alongside with the C_2-C_4 olefins fraction, other liquid hydrocarbons are also produced from the waste plastic which can be further used in other downstream applications or be recycled on top of the reactor to yield light olefins fraction.

[0089] The MESOC+ porous carbon materials display lower light olefins yield and a higher fraction of liquid hydrocarbons ranged from C_5 to C_{20} contributing to about 50 %. The mesoporous carbon materials also display a high stability as a function of cycling tests which also confirms their interest for such process.

[0090] It is worthy to note that on both non-porous and porous carbon materials the production of aromatic compounds is extremely low, at reaction temperature ≤ 500 °C, compared to the linear or branched hydrocarbons which could be due to the lack of strong acidity on such carbon materials unlikely to those existing on zeolite catalysts. Such results are of high interest as aromatics formation contributes to an enhancement of a hydrogen pool which can react with unstable intermediate olefins to yield saturated products. The results obtained have shown that non-porous carbon material with no internal porosity and very low specific surface area, i.e. carbon felt, mostly yields higher light olefins which could be attributed to the high desorption rate of light olefins intermediates on one side, and the lower aromatics formation which lower the hydrogen for hydrogenation of such intermediates. On the other hand, porous carbon which could induce higher residence time, leads to the formation of higher liquid fraction and lower light olefins fraction within the gaseous products.

Reference List

[0091]

1. Onwudili J. A., Muhammad C., Williams P. T. Influence of catalyst bed temperature and properties of zeolite catalysts on pyrolysis-catalysis of a simulated mixed plastics sample for the production of upgraded fuels and chemicals. J. Energ. Inst. 92, 1337-1347 (2019).
2. Lopez G., Artetxe M., Amutio M., Bilbao J., Olazar M. A review on thermal and catalytic pyrolysis of plastic solid waste (PSW). Thermochemical routes for the valorization of waste polyolefinic plastics to produce fuels and chemicals. A review. Renewable Sustainable Energy Rev. 73, 346-368 (2017).
3. Dogu O., Pelucchi M., Van de Vijver R., Van Steenberge P. H. M., D'hooge D. R., Cuoci A., Mehl M., Frassoldati A., Faravelli T., Van Geem K. M. The chemistry of chemical recycling of solid plastic waste via pyrolysis and gasification: state-of-the-art, challenges, and future directions. Prog. Energy Combust. Sci. 84, 100901 (2021).
4. J.-P. Lange, Managing Plastic Waste-Sorting, Recycling, Disposal, and Product Redesign, ACS Sustain. Chem. Eng., 2021, 9, 15722-15738 https://doi.org/10.1021/acssuschemeng.1c05013.
5. Layritz, L. S., Dolganova, I., Finkbeiner, M., Luderer, G., Penteado, A. T., Ueckerdt, F., et al. (2021). The Potential of Direct Steam Cracker Electrification and Carbon Capture & Utilization via Oxidative Coupling of Methane as Decarbonization Strategies for Ethylene Production. Appl. Energ. 296, 117049. doi:10.1016/j.apenergy.2021.117049.
6. Schiffer Z. J., Manthiram K. Electrification and Decarbonization of the Chemical Industry. Joule 1, 10-14 (2017).
7. Jie X., Li W., Slocombe D., Gao Y., Banerjee I., Gonzalez-Cortes S., Yao B., Almegren H., Alshihri S., Dilworth J., Thomas J., Xiao T., Edwards P. Microwave-initiated catalytic deconstruction of plastic waste into hydrogen and high-value carbons. Nat. Catal. 3, 902-912 (2020).
8. Zhou N., Dai L., Lv Y., Li H., Deng W., Guo F., Chen P., Lei H., Ruan R. Catalytic pyrolysis of plastic wastes in a continuous microwave assisted pyrolysis system for fuel production. Chem. Eng. J. 418, 129412 (2021).
9. Wang, W., Tuci, G., Duong-Viet, C., Liu, Y., Rossin, A., Luconi, L., Nhut, J.-M., Nguyen-Dinh, L., Giambastiani, G., Pham-Huu, C., 2019. Induction heating: an enabling technology for the heat management in catalytic processes, ACS Catal., 2019, 9, 7921-7935.Khattak et al., 2019
10. Haneishi N., Tsubaki S., Abe E., Maitani M. M., Suzuki E., Fujii S., Fukushima J., Takizawa H., Wada Y., 2019. Enhancement of fixed-bed flow reactions under microwave irradiation by local heating at the vicinal contact points of catalyst particles. Sci. Rep. 9, 222.
11. Xie W., Yang F., Meng S., Scarpa F., Wang L. 2020 . Perforation of needle-punched carbon-carbon composites during high-temperature and high-velocity ballistic impacts. Composite Structures 245, 112224 (2020).
12. Ali S., Garforth A. A., Harris D. H., Rawlence D. J., Uemichi Y. Polymer waste recycling over "used" catalysts. Catal. Today 75, 247-255 (2002).
13. De La Puente G., Klocker C., Sedran U. Conversion of waste plastics into fuels recycling polyethylene in FCC. Appl. Catal. B Environ. 36, 279-285 (2002).
14. Lin Y., Yang M. Catalytic conversion of commingled polymer waste into chemicals and fuels over spent FCC commercial catalyst in fluidised-bed reactor. Appl. Catal. B Environ. 69, 145-153 (2007).
15. Olazar M., Lopez G., Amutio M., Elordi G., Aguado R., Bilbao J. Influence of FCC catalyst steaming on HDPE pyrolysis product distribution. J. Anal. Appl. Pyrol. 85, 359-365 (2009).
16. Elordi G., Olazar M., Castano P., Artextxe M., Bilbao J. Polyethylene cracking on a spent FCC catalyst in a conical spouted bed. Ind. Eng. Chem. Res. 51, 14008-14017 (2012).
17. Eschenbacher A., Varghese R. J., Abbas-Abadi M. S., Van Geem K. M. Maximizing light olefins and aromatics

as high value base chemicals via single step catalytic conversion of plastic waste. Chem. Eng. J. 428, 132087 (2022).

Claims

1. Use of a metal-free carbon material for converting plastic into C_2-C_4 olefins and/or other hydrocarbons, under direct induction heating at temperature less than or equal to 800 °C.

2. Use according to claim 1, wherein said metal-free carbon material has a BET surface area of at least 0.10 m^2/g and up to 2000 m^2/g, as determined by ASTM-D-3663 (2020).

3. Use according to claim 1 or 2, wherein said metal-free carbon material is selected from the group comprising graphite, graphene, mesoporous carbon, carbon black, acetylene black, pyrolytic carbon, activated carbon and any combinations thereof.

4. Use according to anyone of claims 2 to 3, wherein said metal-free carbon material has a morphology chosen among grain, felt, fiber, for example nanofiber, filament, 2D or 3D fabrics, foam as open cell foam, 3D-printed structures, sphere, cloth, monolith as honeycombs, extrudates, rodshaped, sticks and particles, tube, for example nanotube, ring or trilobes, tablets and nanotablets and any combinations thereof.

5. Use according to anyone of the preceding claims, wherein said metal-free carbon material is supported by a non-carbon structure.

6. Process for converting plastic into C_2-C_4 olefin and/or other hydrocarbons, comprising a step of reaction under direct induction heating, with a metal-free carbon material as defined in anyone of the preceding claims, at temperature less than or equal to 800 °C.

7. Process according to claim 6, wherein plastic is vaporized in a first-stage reactor, while vapors generated in the first section are swept with a gas flow toward the material in a second-stage reactor where the cracking process takes place.

8. Use according to claims 1 to 5, or process according to claim 6 or 7, wherein said plastic is at least one plastic selected among high and low-density polyethylene, polypropylene, polystyrene, mixed industrial waste plastic, as low-density polyethylene, PET, PVC and polystyrene containing solid residue and plastics containing solid residue.

9. Use or process according to claim 8, wherein said C_2-C_4 olefins, comprising possibility traces of diolefins, are ethylene and/or propylene, and said other hydrocarbons are C_{5+} liquid hydrocarbons and/or paraffinic gaseous C_1 to C_4 hydrocarbons.

10. Use or process according to claim 8 or 9, wherein said C_5, liquid hydrocarbon is fuel.

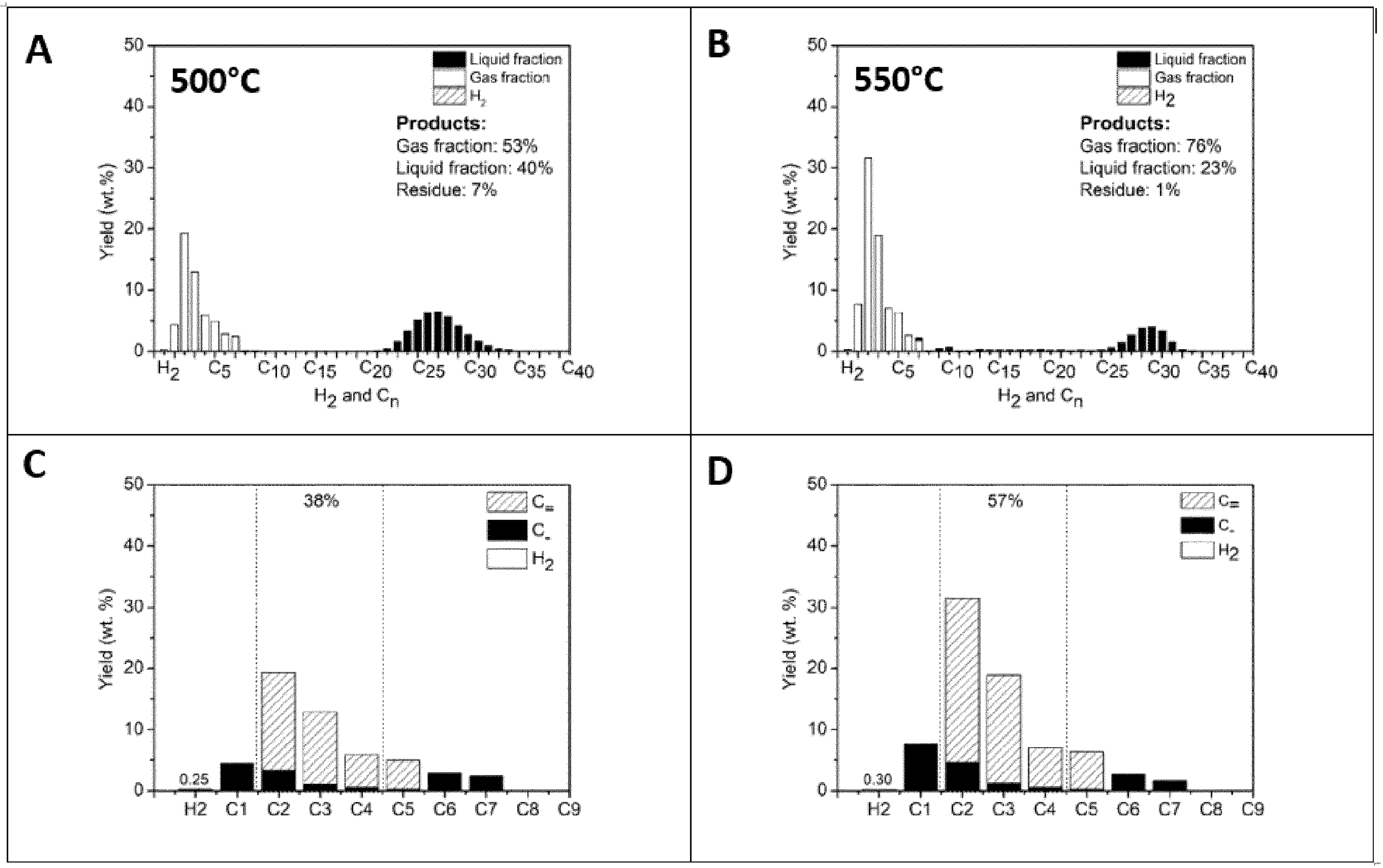
A
500°C
Liquid fraction
Gas fraction
H_2
Products:
Gas fraction: 53%
Liquid fraction: 40%
Residue: 7%
Yield (wt.%)
0
10
20
30
40
50
H_2
C_5
C_{10}
C_{15}
C_{20}
C_{25}
C_{30}
C_{35}
C_{40}
H_2 and C_n
B
550°C
Liquid fraction
Gas fraction
H_2
Products:
Gas fraction: 76%
Liquid fraction: 23%
Residue: 1%
Yield (wt.%)
0
10
20
30
40
50
H_2
C_5
C_{10}
C_{15}
C_{20}
C_{25}
C_{30}
C_{35}
C_{40}
H_2 and C_n
C
38%
$C_=$
C_-
H_2
Yield (wt. %)
0
10
20
30
40
50
0.25
H2
C1
C2
C3
C4
C5
C6
C7
C8
C9
D
57%
$C_=$
C_-
H_2
Yield (wt. %)
0
10
20
30
40
50
0.30
H2
C1
C2
C3
C4
C5
C6
C7
C8
C9

Figure 1

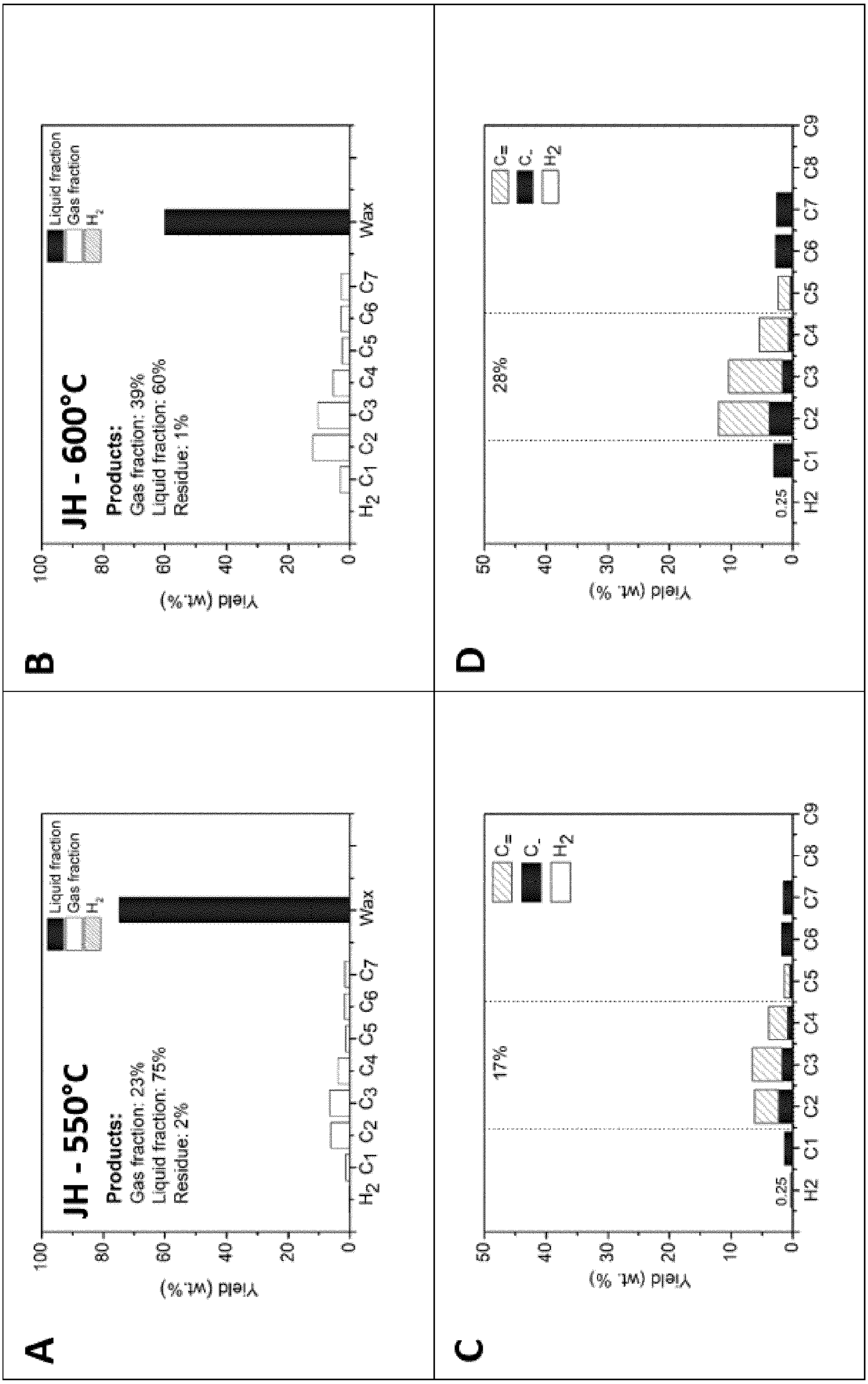
A
JH - 550°C
Products:
Gas fraction: 23%
Liquid fraction: 75%
Residue: 2%
Liquid fraction
Gas fraction
H2
Yield (wt.%)
0
20
40
60
80
100
H2 C1 C2 C3 C4 C5 C6 C7
Wax
B
JH - 600°C
Products:
Gas fraction: 39%
Liquid fraction: 60%
Residue: 1%
Liquid fraction
Gas fraction
H2
Yield (wt.%)
0
20
40
60
80
100
H2 C1 C2 C3 C4 C5 C6 C7
Wax
C
17%
0.25
C=
C-
H2
Yield (wt. %)
0
10
20
30
40
50
H2
C1
C2
C3
C4
C5
C6
C7
C8
C9
D
28%
0.25
C=
C-
H2
Yield (wt. %)
0
10
20
30
40
50
H2
C1
C2
C3
C4
C5
C6
C7
C8
C9

Figure 2

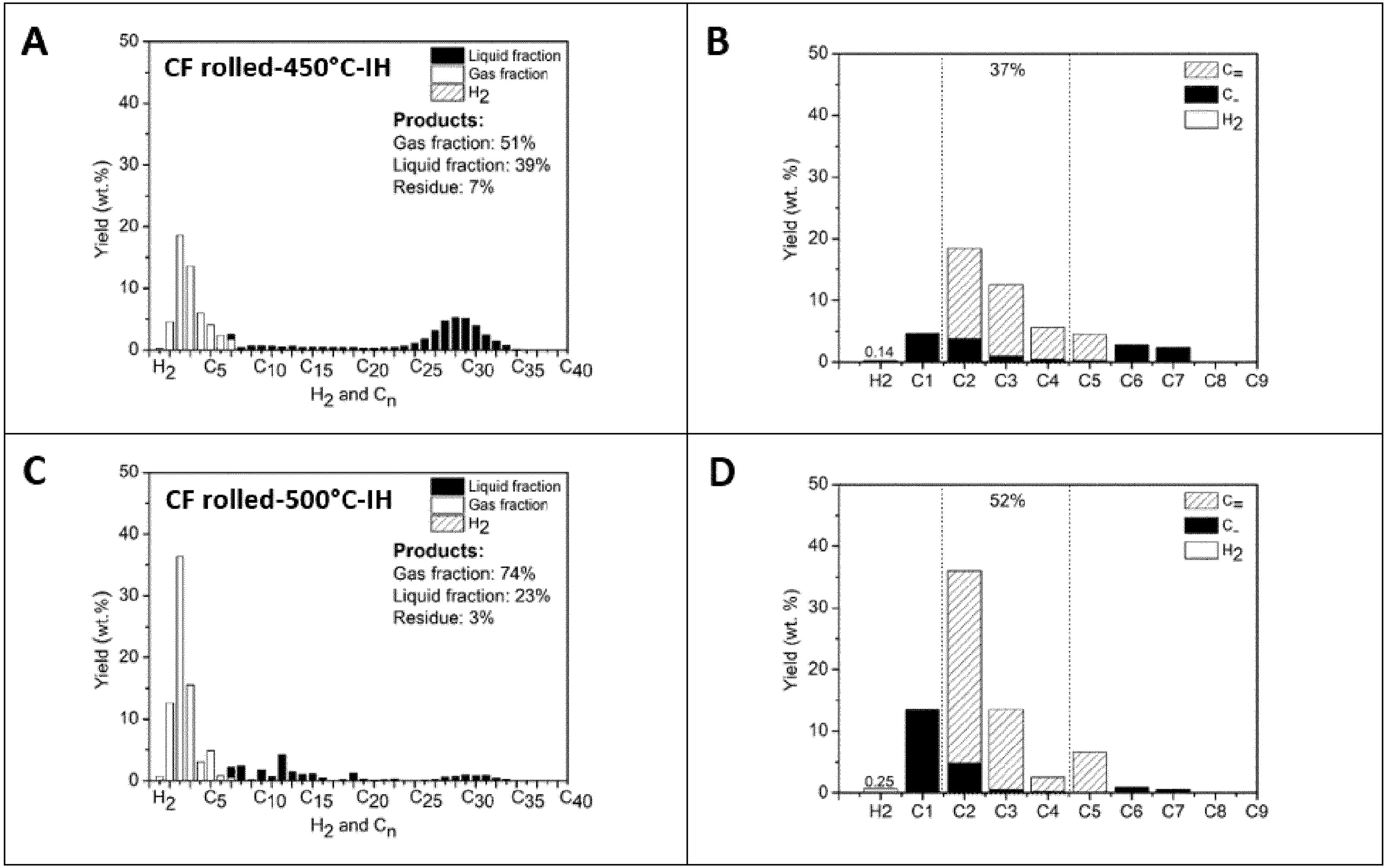

Figure 3 (A, B, C, D)

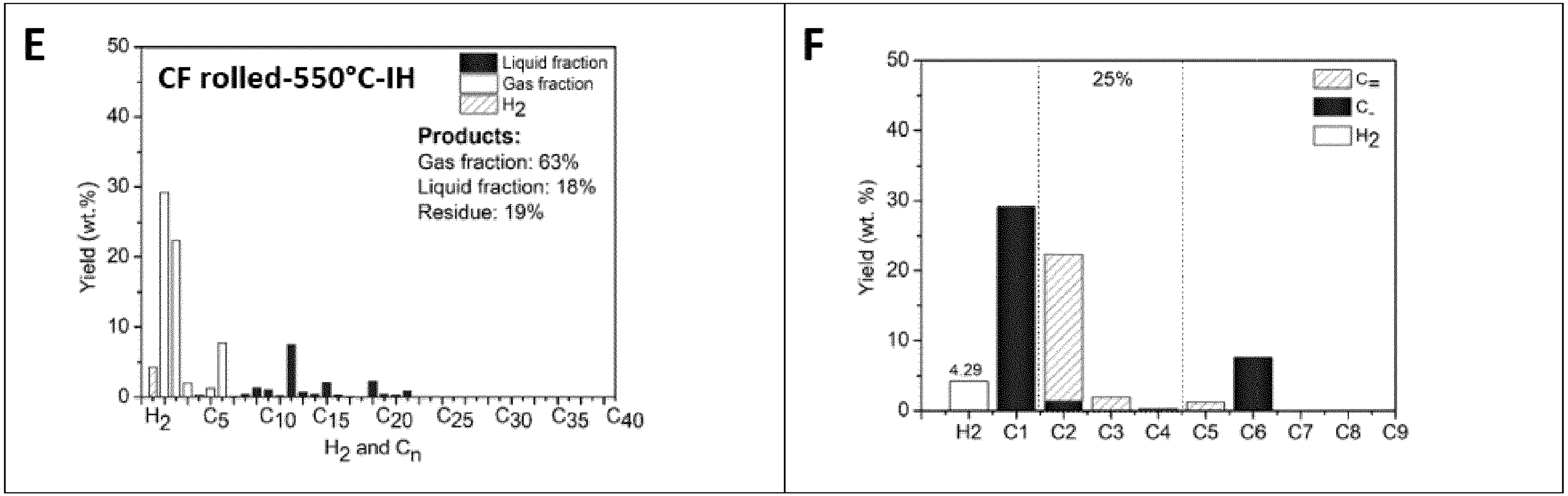
E
CF rolled-550°C-IH
Liquid fraction
Gas fraction
H_2
Products:
Gas fraction: 63%
Liquid fraction: 18%
Residue: 19%
Yield (wt.%)
0
10
20
30
40
50
H_2
C_5
C_{10}
C_{15}
C_{20}
C_{25}
C_{30}
C_{35}
C_{40}
H_2 and C_n
F
25%
$C_=$
C_-
H_2
Yield (wt. %)
0
10
20
30
40
50
4.29
H2
C1
C2
C3
C4
C5
C6
C7
C8
C9

Figure 3 (E, F)

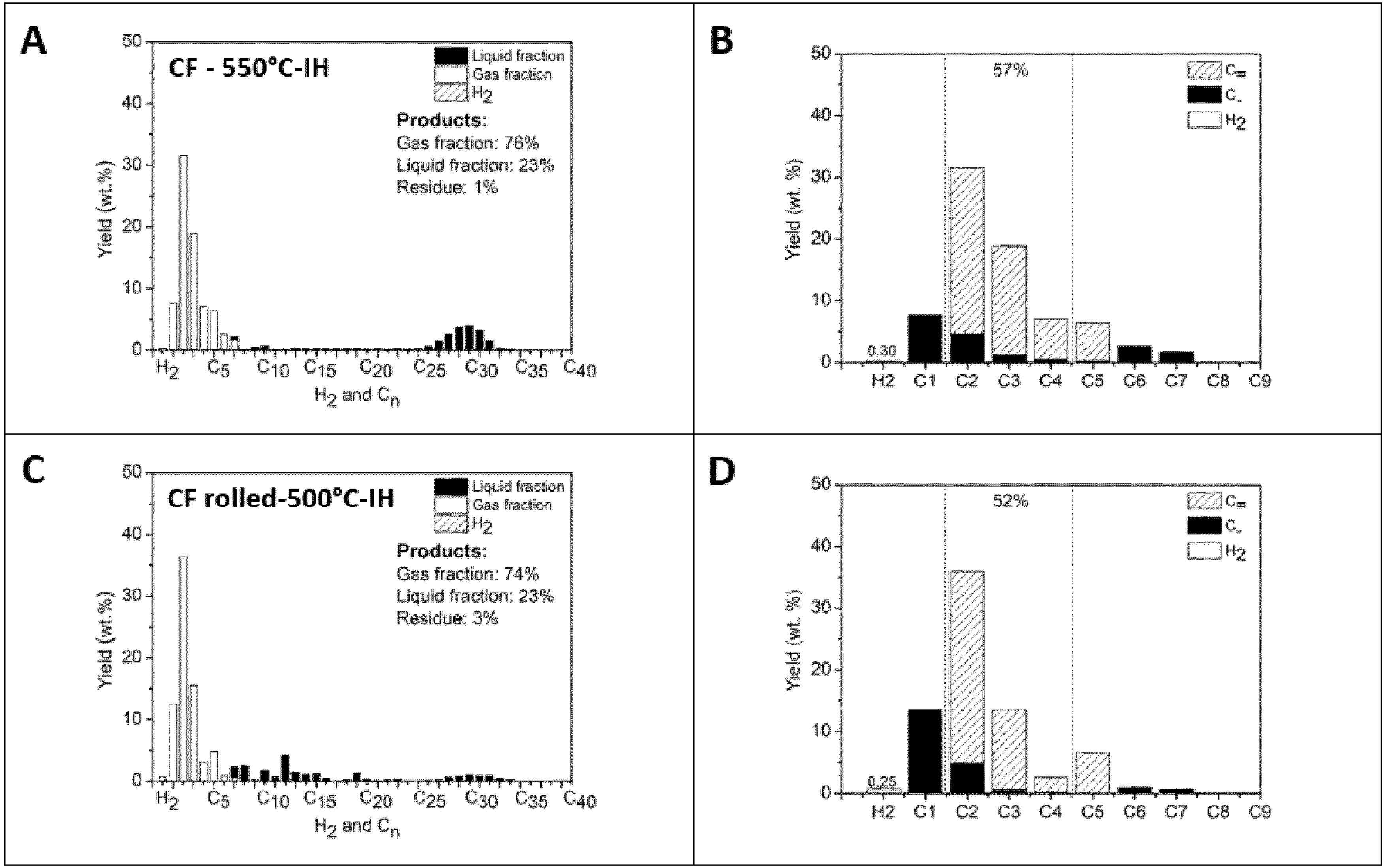
A
CF - 550°C-IH
Liquid fraction
Gas fraction
H_2
Products:
Gas fraction: 76%
Liquid fraction: 23%
Residue: 1%
Yield (wt.%)
50
40
30
20
10
0
H_2
C_5
C_{10}
C_{15}
C_{20}
C_{25}
C_{30}
C_{35}
C_{40}
H_2 and C_n
B
Yield (wt. %)
50
40
30
20
10
0
57%
0.30
$C_=$
C_-
H_2
H2
C1
C2
C3
C4
C5
C6
C7
C8
C9
C
CF rolled-500°C-IH
Liquid fraction
Gas fraction
H_2
Products:
Gas fraction: 74%
Liquid fraction: 23%
Residue: 3%
Yield (wt.%)
50
40
30
20
10
0
H_2
C_5
C_{10}
C_{15}
C_{20}
C_{25}
C_{30}
C_{35}
C_{40}
H_2 and C_n
D
Yield (wt. %)
50
40
30
20
10
0
52%
0.25
$C_=$
C_-
H_2
H2
C1
C2
C3
C4
C5
C6
C7
C8
C9

Figure 4

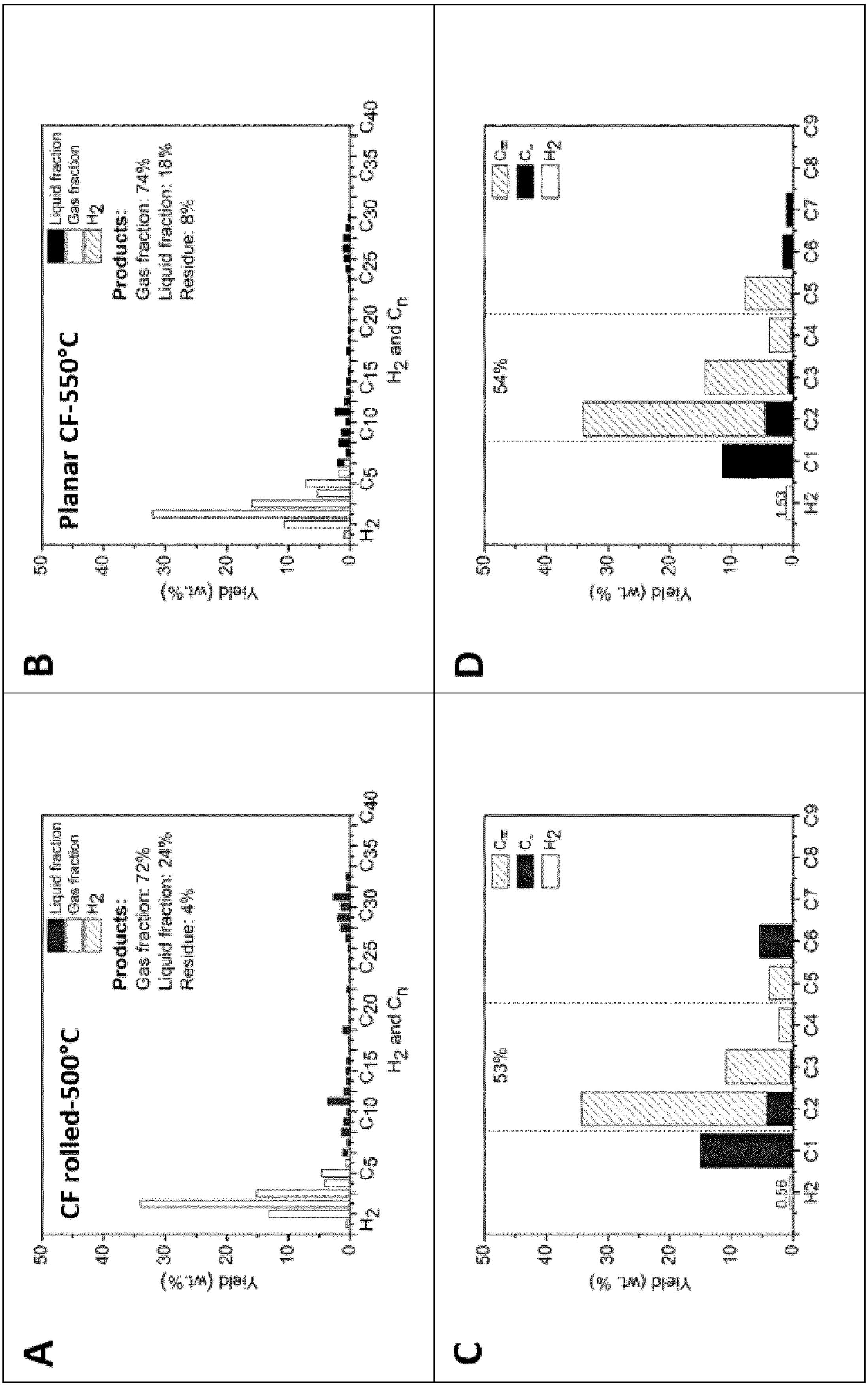
A
CF rolled-500°C
Liquid fraction
Gas fraction
H_2
Products:
Gas fraction: 72%
Liquid fraction: 24%
Residue: 4%
Yield (wt.%)
0
10
20
30
40
50
H_2
C_5
C_{10}
C_{15}
C_{20}
C_{25}
C_{30}
C_{35}
C_{40}
H_2 and C_n
B
Planar CF-550°C
Liquid fraction
Gas fraction
H_2
Products:
Gas fraction: 74%
Liquid fraction: 18%
Residue: 8%
Yield (wt.%)
0
10
20
30
40
50
H_2
C_5
C_{10}
C_{15}
C_{20}
C_{25}
C_{30}
C_{35}
C_{40}
H_2 and C_n
C
53%
0.56
C=
C-
H2
Yield (wt. %)
0
10
20
30
40
50
H2
C1
C2
C3
C4
C5
C6
C7
C8
C9
D
54%
1.53
C=
C-
H2
Yield (wt. %)
0
10
20
30
40
50
H2
C1
C2
C3
C4
C5
C6
C7
C8
C9

Figure 5

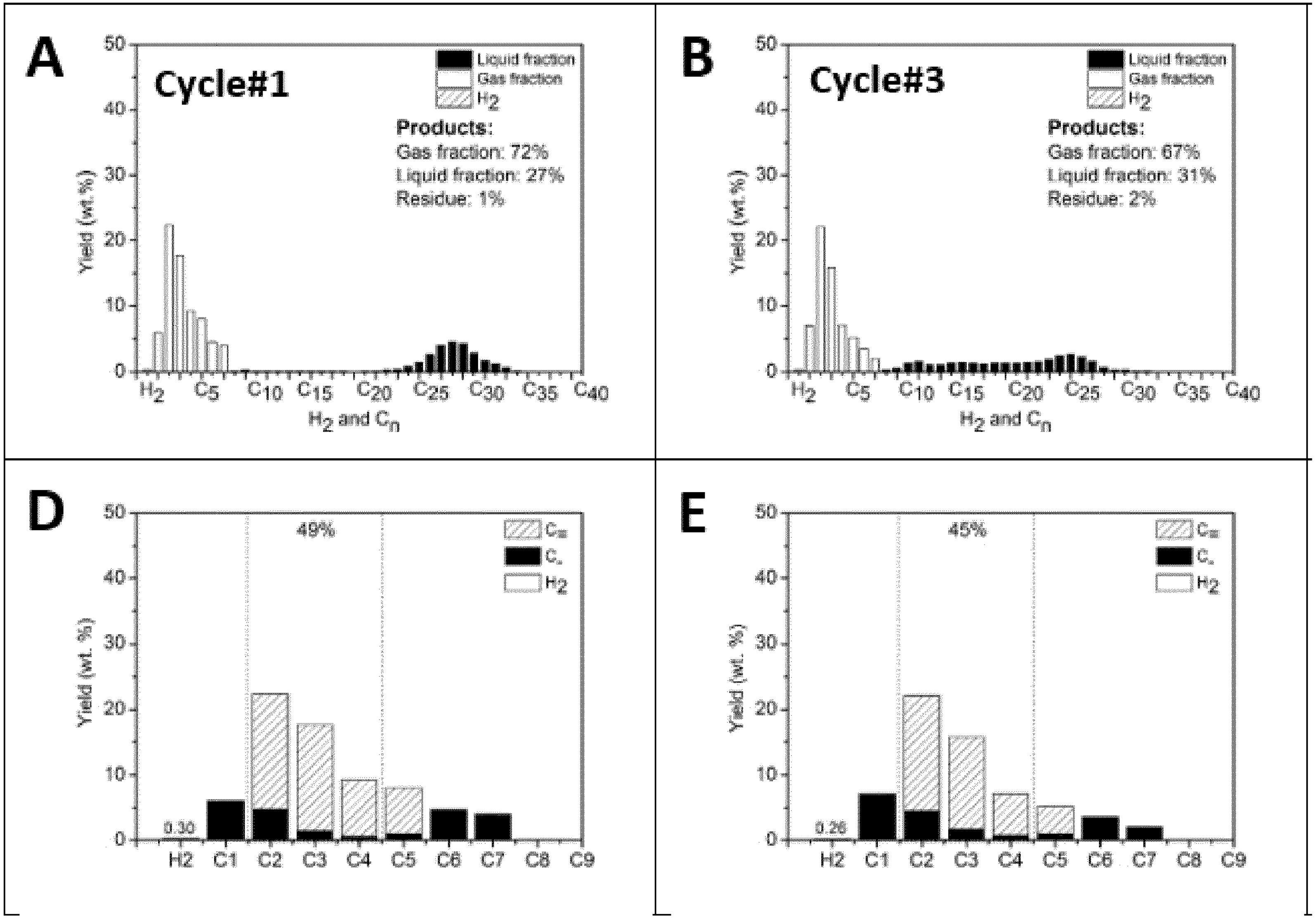

Figure 6 (A, B, D, E)

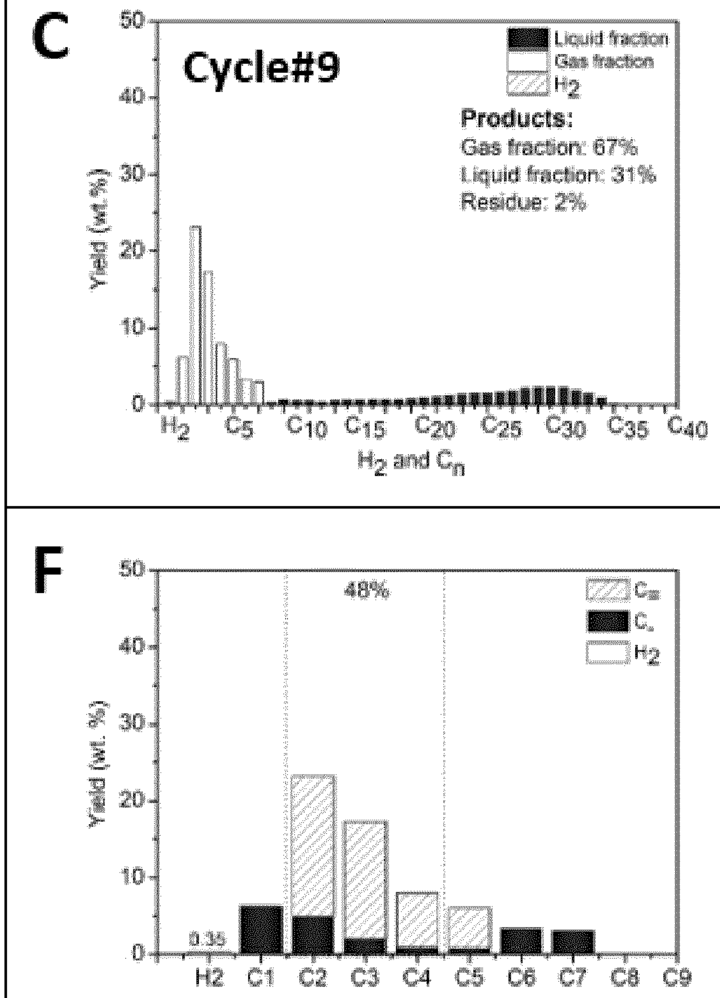
C
Cycle#9
Liquid fraction
Gas fraction
H_2
Products:
Gas fraction: 67%
Liquid fraction: 31%
Residue: 2%
Yield (wt.%)
0
10
20
30
40
50
H_2
C_5
C_{10}
C_{15}
C_{20}
C_{25}
C_{30}
C_{35}
C_{40}
H_2 and C_n
F
48%
$C_=$
C_-
H_2
Yield (wt. %)
0.35
0
10
20
30
40
50
H2
C1
C2
C3
C4
C5
C6
C7
C8
C9

Figure 6 (C, F)

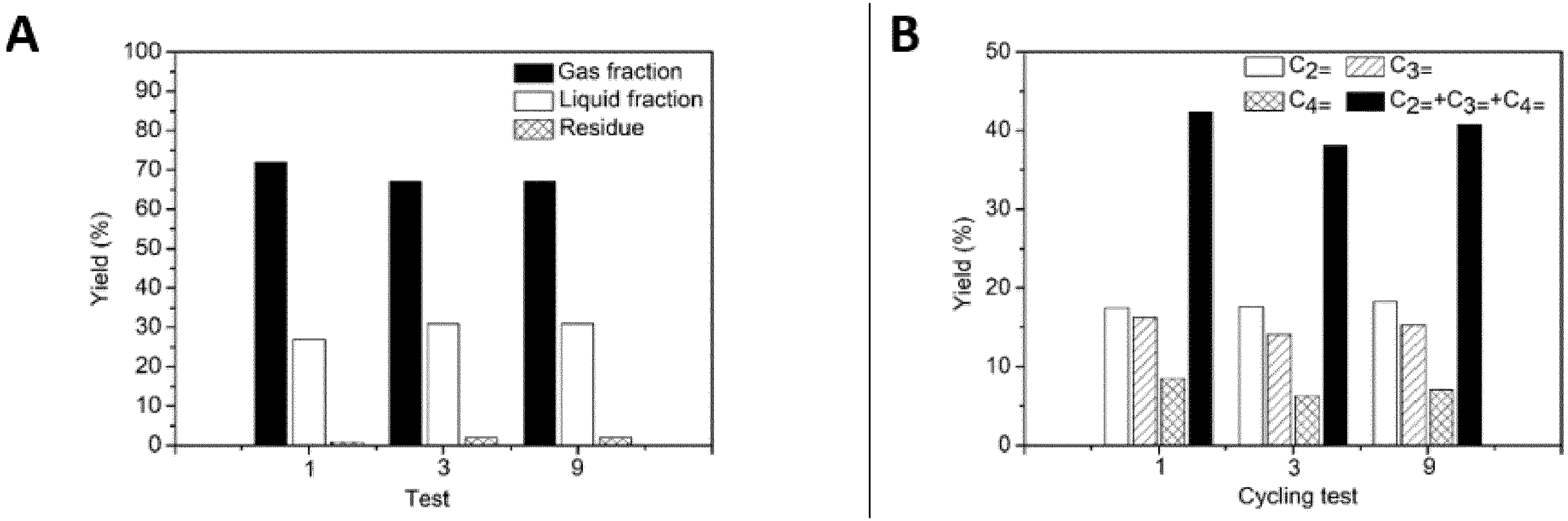
A
Yield (%)
100
90
80
70
60
50
40
30
20
10
0
1
3
9
Test
Gas fraction
Liquid fraction
Residue
B
Yield (%)
50
40
30
20
10
0
1
3
9
Cycling test
$C_{2=}$
$C_{3=}$
$C_{4=}$
$C_{2=}+C_{3=}+C_{4=}$

Figure 7

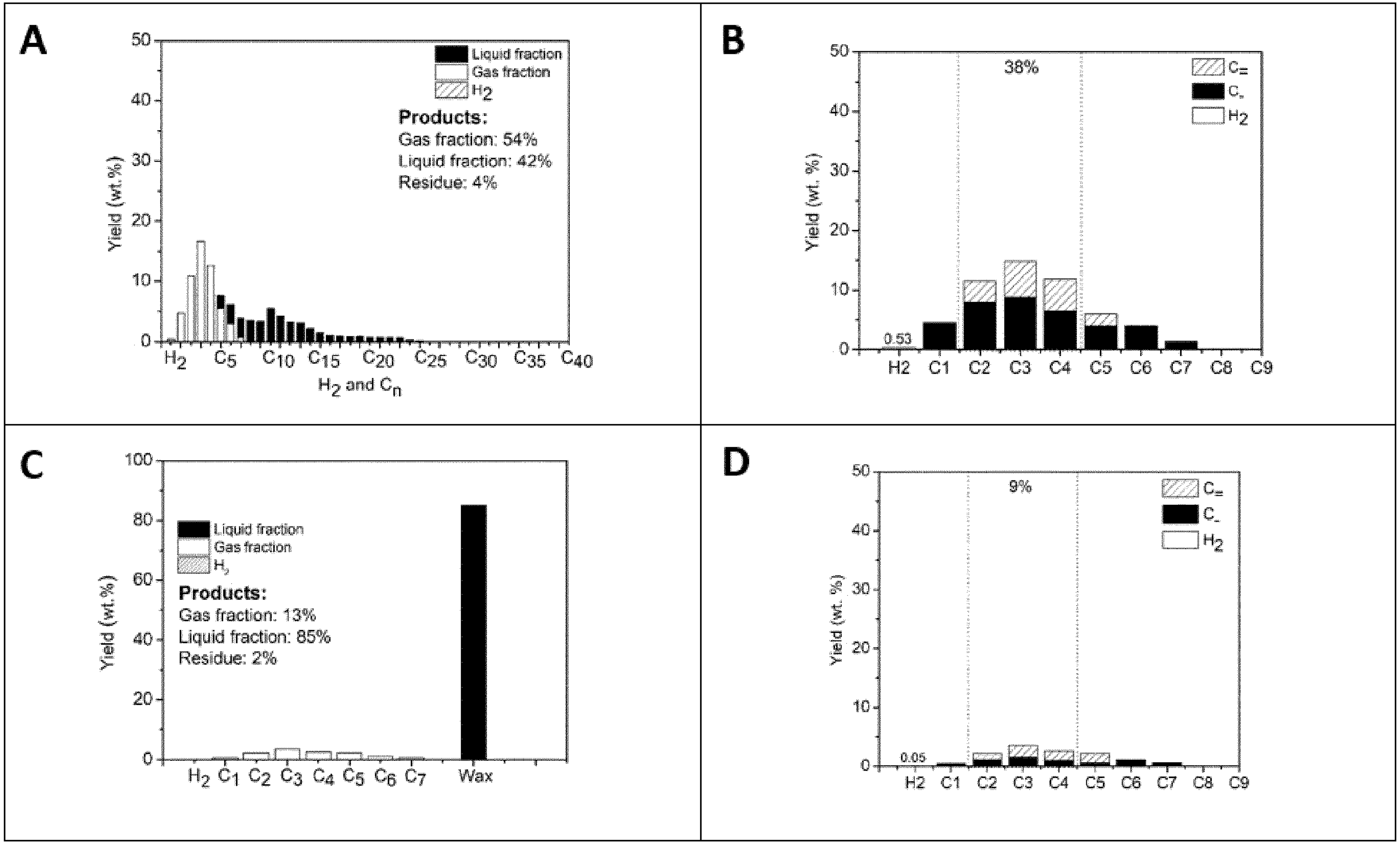

Figure 8 (A, B, C, D)

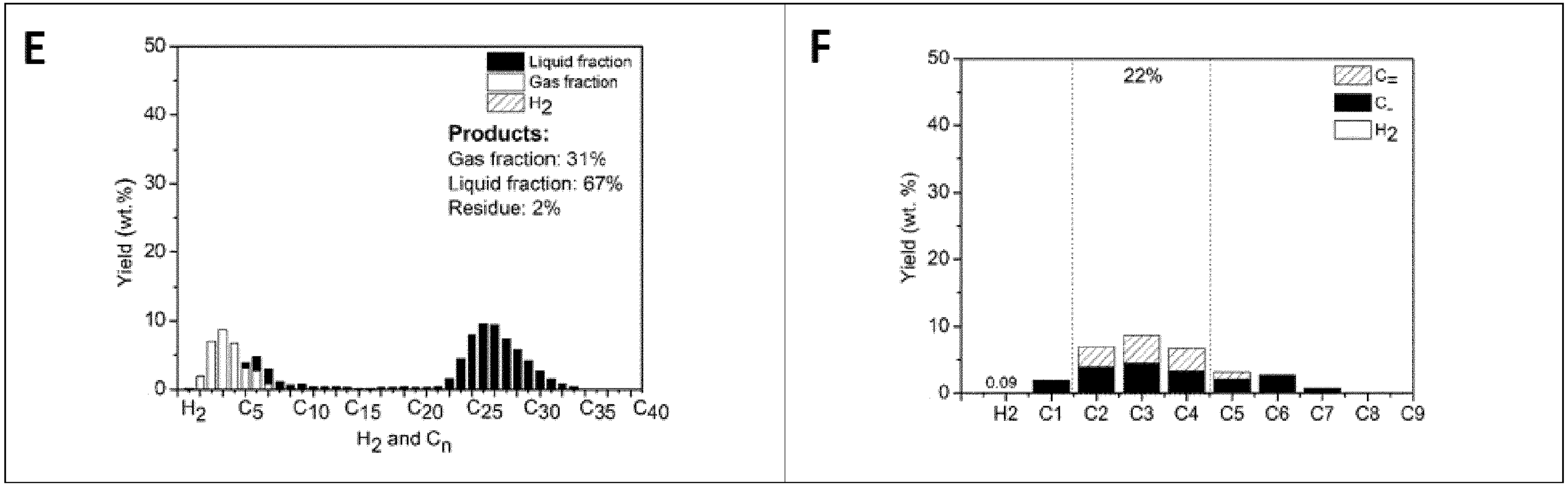
E
Yield (wt.%)
50
40
30
20
10
0
H_2
C_5
C_{10}
C_{15}
C_{20}
C_{25}
C_{30}
C_{35}
C_{40}
H_2 and C_n
Liquid fraction
Gas fraction
H_2
Products:
Gas fraction: 31%
Liquid fraction: 67%
Residue: 2%
F
Yield (wt. %)
50
40
30
20
10
0
H2
C1
C2
C3
C4
C5
C6
C7
C8
C9
0.09
22%
$C_=$
C_-
H_2

Figure 8 (E, F)

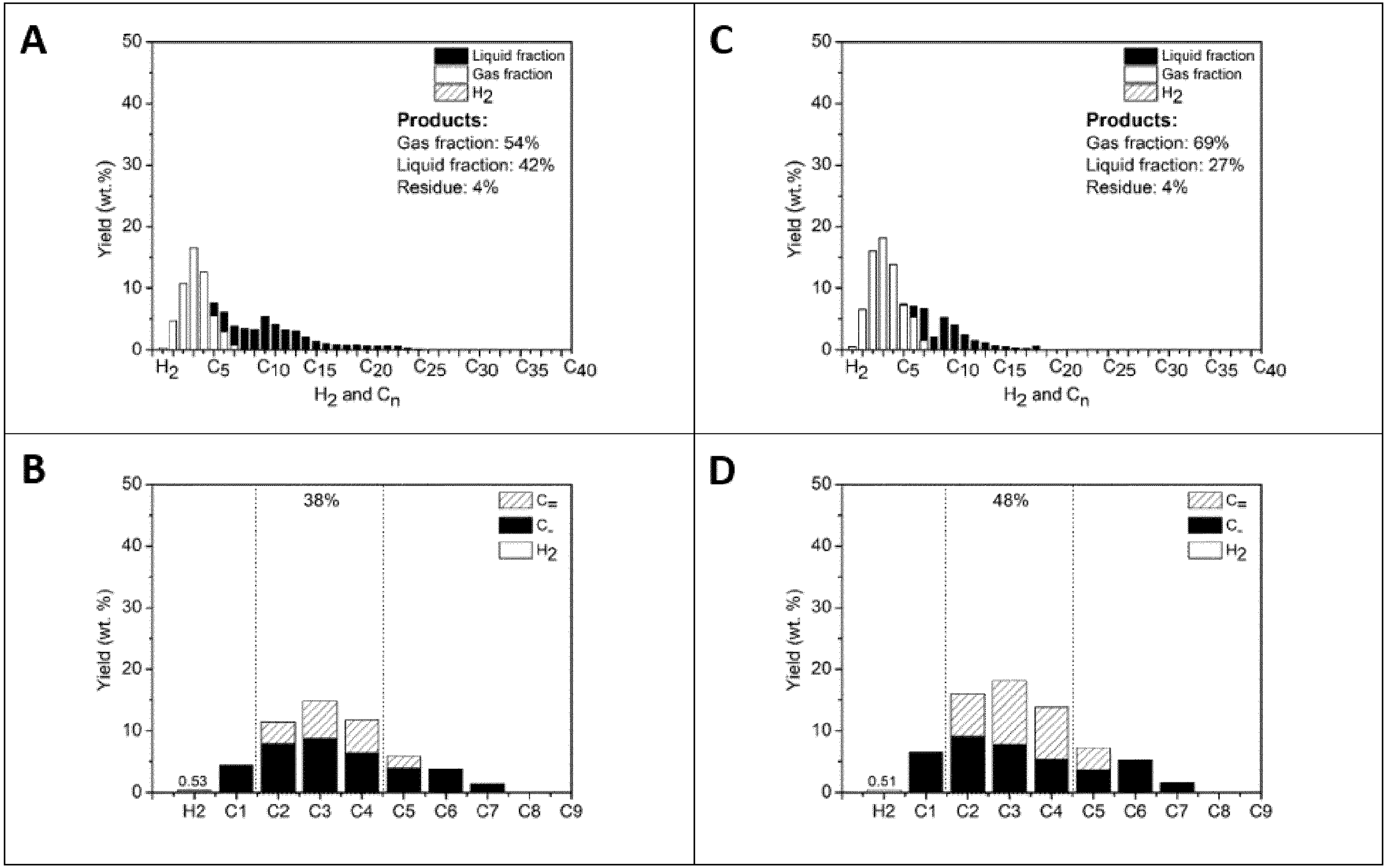
A
Yield (wt.%)
50
40
30
20
10
0
H_2
C_5
C_{10}
C_{15}
C_{20}
C_{25}
C_{30}
C_{35}
C_{40}
H_2 and C_n
Liquid fraction
Gas fraction
H_2
Products:
Gas fraction: 54%
Liquid fraction: 42%
Residue: 4%
C
Yield (wt.%)
50
40
30
20
10
0
H_2
C_5
C_{10}
C_{15}
C_{20}
C_{25}
C_{30}
C_{35}
C_{40}
H_2 and C_n
Liquid fraction
Gas fraction
H_2
Products:
Gas fraction: 69%
Liquid fraction: 27%
Residue: 4%
B
Yield (wt. %)
50
40
30
20
10
0
38%
$C_=$
C_-
H_2
0.53
H2
C1
C2
C3
C4
C5
C6
C7
C8
C9
D
Yield (wt. %)
50
40
30
20
10
0
48%
$C_=$
C_-
H_2
0.51
H2
C1
C2
C3
C4
C5
C6
C7
C8
C9

Figure 9

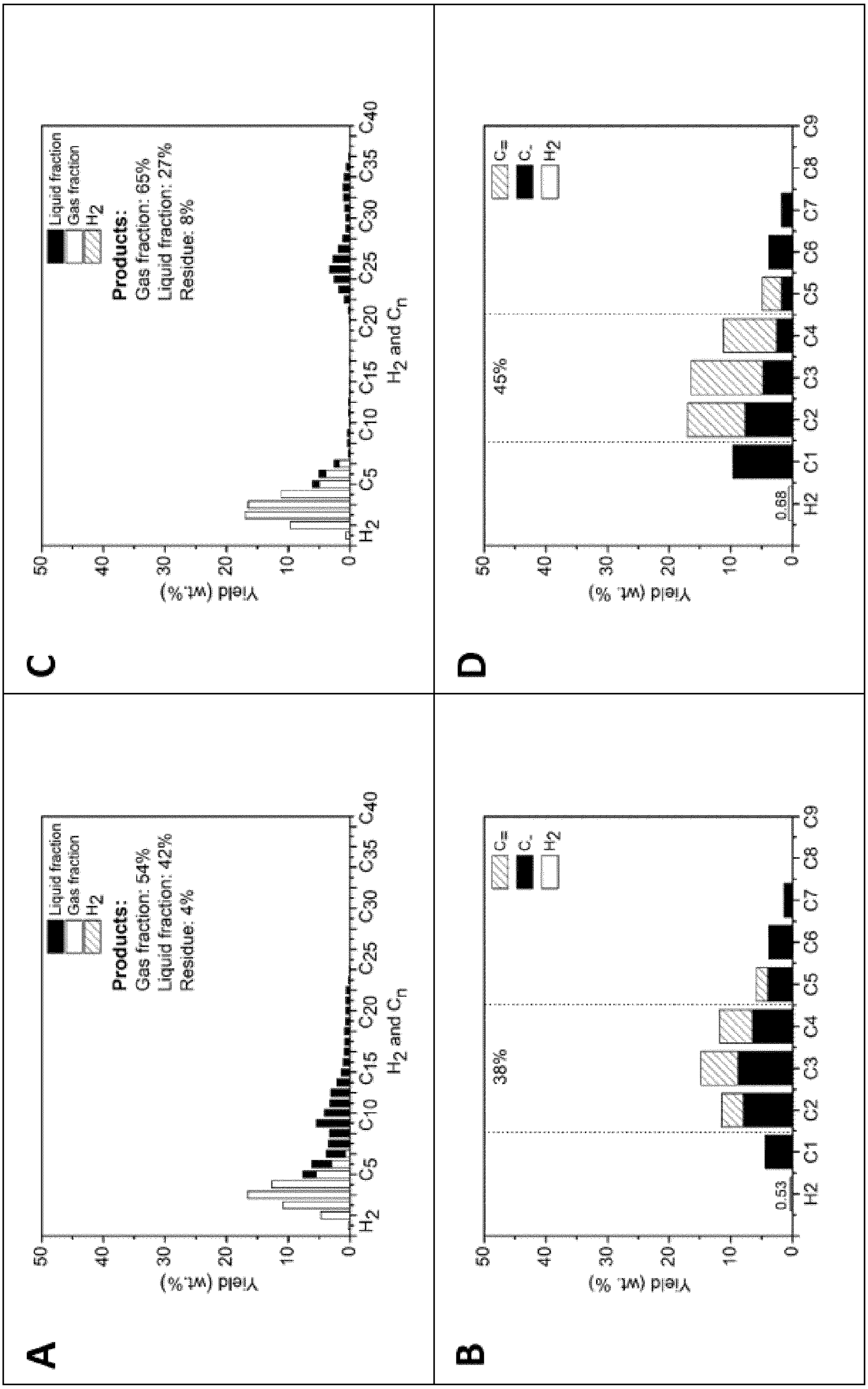
A
Yield (wt.%)
50
40
30
20
10
0
H2
C5
C10
C15
C20
C25
C30
C35
C40
H2 and Cn
Liquid fraction
Gas fraction
H2
Products:
Gas fraction: 54%
Liquid fraction: 42%
Residue: 4%
B
Yield (wt. %)
0.53
38%
H2
C1
C2
C3
C4
C5
C6
C7
C8
C9
C=
C-
H2
C
Products:
Gas fraction: 65%
Liquid fraction: 27%
Residue: 8%
D
0.68
45%

Figure 10

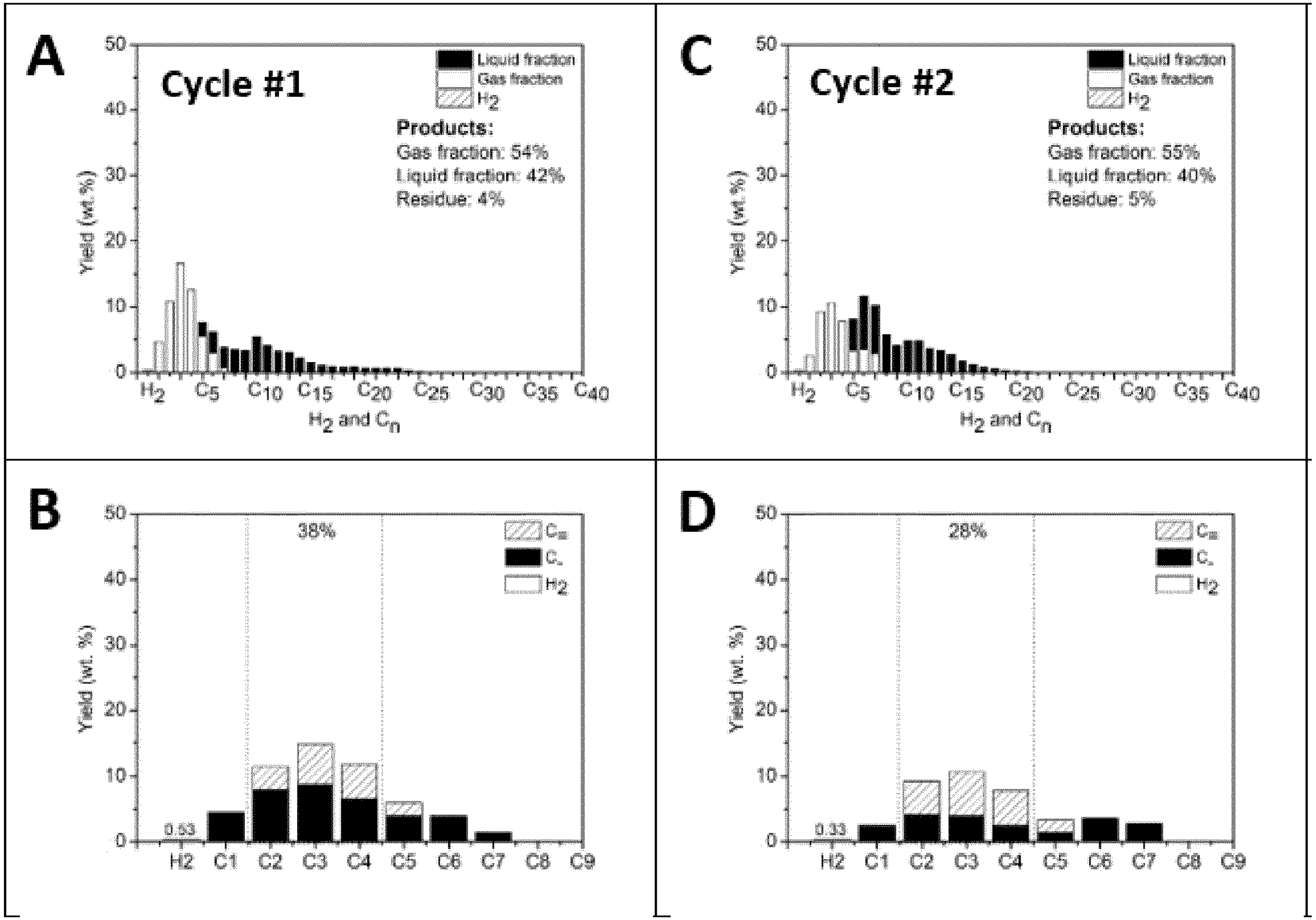

Figure 11 (A, B, C, D)

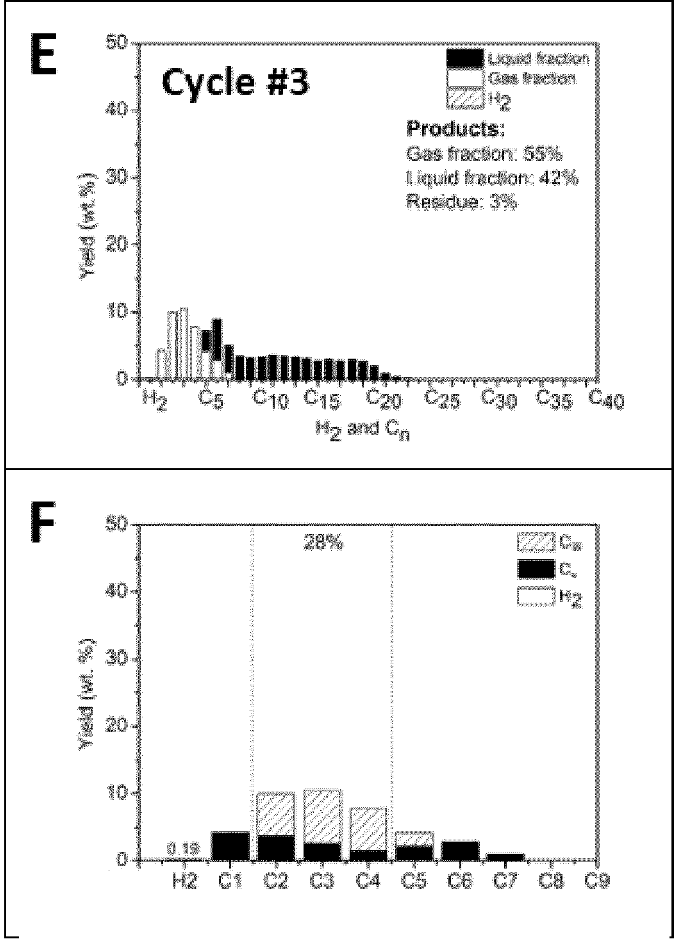
E
Cycle #3
Liquid fraction
Gas fraction
H2
Products:
Gas fraction: 55%
Liquid fraction: 42%
Residue: 3%
Yield (wt.%)
50
40
30
20
10
0
H2
C5
C10
C15
C20
C25
C30
C35
C40
H2 and Cn
F
28%
C=
C-
H2
Yield (wt. %)
50
40
30
20
10
0
0.19
H2
C1
C2
C3
C4
C5
C6
C7
C8
C9

Figure 11 (E, F)

Europäisches Patentamt
European Patent Office
Office européen des brevets

EUROPEAN SEARCH REPORT

Application Number
EP 22 30 6835

DOCUMENTS CONSIDERED TO BE RELEVANT

Category	Citation of document with indication, where appropriate, of relevant passages	Relevant to claim	CLASSIFICATION OF THE APPLICATION (IPC)
X	US 2022/154074 A1 (GUSLISTY ALEXANDER [GB]) 19 May 2022 (2022-05-19) * paragraphs [0042], [0054], [0057], [0061] * * figures 1-10 * * claims 1-21 * -----	1-10	INV. C10B19/00 C10B53/07 C10G1/10 H05B6/10
X	US 2016/075953 A1 (MAXWELL ANDREW JAMES [US] ET AL) 17 March 2016 (2016-03-17) * figures 1-9 * * claims 17-20 * * paragraphs [0062], [0167], [0168] * * claims 1-20 * -----	1-10	
A	JP H11 302663 A (JAPAN STEEL WORKS LTD) 2 November 1999 (1999-11-02) * figures 1-3 * * paragraphs [0022], [0023] * * example * -----	1-10	
			TECHNICAL FIELDS SEARCHED (IPC)
			C10B C10G H05B C08J

The present search report has been drawn up for all claims

Place of search	Date of completion of the search	Examiner
The Hague	31 May 2023	Zuurdeeg, Boudewijn

1

CATEGORY OF CITED DOCUMENTS

X : particularly relevant if taken alone
Y : particularly relevant if combined with another document of the same category
A : technological background
O : non-written disclosure
P : intermediate document

T : theory or principle underlying the invention
E : earlier patent document, but published on, or after the filing date
D : document cited in the application
L : document cited for other reasons
....
& : member of the same patent family, corresponding document

ANNEX TO THE EUROPEAN SEARCH REPORT ON EUROPEAN PATENT APPLICATION NO.

EP 22 30 6835

31-05-2023

Patent document cited in search report	Publication date	Patent family member(s)	Publication date
US 2022154074 A1	19-05-2022	CN 113784783 A	10-12-2021
		EP 3956052 A1	23-02-2022
		GB 2583097 A	21-10-2020
		US 2022154074 A1	19-05-2022
		WO 2020212274 A1	22-10-2020
US 2016075953 A1	17-03-2016	NONE	
JP H11302663 A	02-11-1999	NONE	

EPO FORM P0459

For more details about this annex : see Official Journal of the European Patent Office, No. 12/82

REFERENCES CITED IN THE DESCRIPTION

Non-patent literature cited in the description

- **J.-P. LANGE.** Managing Plastic Waste-Sorting, Recycling, Disposal, and Product Redesign. *ACS Sustain. Chem. Eng.,* 2021, vol. 9, 15722-15738, https://doi.org/10.1021/acssuschemeng.1c05013 **[0008] [0091]**
- **Y. ZHANG ; D. DUAN ; H. LEI ; E. VILLOTA ; R. RUAN.** Jet fuel production from waste plastics via catalytic pyrolysis with activated carbons. *Appl. Energy,* 2019, vol. 251, 113337 **[0011]**
- **ONWUDILI J. A. ; MUHAMMAD C. ; WILLIAMS P. T.** Influence of catalyst bed temperature and properties of zeolite catalysts on pyrolysis-catalysis of a simulated mixed plastics sample for the production of upgraded fuels and chemicals. *J. Energ. Inst.,* 2019, vol. 92, 1337-1347 **[0091]**
- **LOPEZ G. ; ARTETXE M. ; AMUTIO M. ; BILBAO J. ; OLAZAR M.** A review on thermal and catalytic pyrolysis of plastic solid waste (PSW). Thermochemical routes for the valorization of waste polyolefinic plastics to produce fuels and chemicals. *Renewable Sustainable Energy Rev.,* 2017, vol. 73, 346-368 **[0091]**
- **DOGU O. ; PELUCCHI M. ; VAN DE VIJVER R. ; VAN STEENBERGE P. H. M. ; D'HOOGE D. R. ; CUOCI A. ; MEHL M. ; FRASSOLDATI A. ; FARAVELLI T. ; VAN GEEM K. M.** The chemistry of chemical recycling of solid plastic waste via pyrolysis and gasification: state-of-the-art, challenges, and future directions. *Prog. Energy Combust. Sci.,* 2021, vol. 84, 100901 **[0091]**
- **LAYRITZ, L. S. ; DOLGANOVA, I. ; FINKBEINER, M. ; LUDERER, G. ; PENTEADO, A. T. ; UECKERDT, F. et al.** The Potential of Direct Steam Cracker Electrification and Carbon Capture & Utilization via Oxidative Coupling of Methane as Decarbonization Strategies for Ethylene Production. *Appl. Energ.,* 2021, vol. 296, 117049 **[0091]**
- **SCHIFFER Z. J. ; MANTHIRAM K.** Electrification and Decarbonization of the Chemical Industry. *Joule,* 2017, vol. 1, 10-14 **[0091]**
- **JIE X. ; LI W. ; SLOCOMBE D. ; GAO Y. ; BANERJEE I. ; GONZALEZ-CORTES S. ; YAO B. ; ALMEGREN H. ; ALSHIHRI S. ; DILWORTH J.** Microwave-initiated catalytic deconstruction of plastic waste into hydrogen and high-value carbons. *Nat. Catal.,* 2020, vol. 3, 902-912 **[0091]**
- **ZHOU N. ; DAI L. ; LV Y. ; LI H. ; DENG W. ; GUO F. ; CHEN P. ; LEI H. ; RUAN R.** Catalytic pyrolysis of plastic wastes in a continuous microwave assisted pyrolysis system for fuel production. *Chem. Eng. J.,* 2021, vol. 418, 129412 **[0091]**
- **WANG, W. ; TUCI, G. ; DUONG-VIET, C. ; LIU, Y. ; ROSSIN, A. ; LUCONI, L. ; NHUT, J.-M. ; NGUYEN-DINH, L. ; GIAMBASTIANI, G. ; PHAM-HUU, C.** Induction heating: an enabling technology for the heat management in catalytic processes. *ACS Catal.,* 2019, vol. 9, 7921-7935 **[0091]**
- **HANEISHI N. ; TSUBAKI S. ; ABE E. ; MAITANI M. M. ; SUZUKI E. ; FUJII S. ; FUKUSHIMA J. ; TAKIZAWA H. ; WADA Y.** Enhancement of fixed-bed flow reactions under microwave irradiation by local heating at the vicinal contact points of catalyst particles. *Sci. Rep.,* 2019, vol. 9, 222 **[0091]**
- **XIE W. ; YANG F. ; MENG S. ; SCARPA F. ; WANG L.** Perforation of needle-punched carbon-carbon composites during high-temperature and high-velocity ballistic impacts. *Composite Structures,* 2020, vol. 245, 112224 **[0091]**
- **ALI S. ; GARFORTH A. A. ; HARRIS D. H. ; RAWLENCE D. J. ; UEMICHI Y.** Polymer waste recycling over ''used'' catalysts. *Catal. Today,* 2002, vol. 75, 247-255 **[0091]**
- **DE LA PUENTE G. ; KLOCKER C. ; SEDRAN U.** Conversion of waste plastics into fuels recycling polyethylene in FCC. *Appl. Catal. B Environ.,* 2002, vol. 36, 279-285 **[0091]**
- **LIN Y. ; YANG M.** Catalytic conversion of commingled polymer waste into chemicals and fuels over spent FCC commercial catalyst in fluidised-bed reactor. *Appl. Catal. B Environ.,* 2007, vol. 69, 145-153 **[0091]**
- **OLAZAR M. ; LOPEZ G. ; AMUTIO M. ; ELORDI G. ; AGUADO R. ; BILBAO J.** Influence of FCC catalyst steaming on HDPE pyrolysis product distribution. *J. Anal. Appl. Pyrol.,* 2009, vol. 85, 359-365 **[0091]**
- **ELORDI G. ; OLAZAR M. ; CASTANO P. ; ARTEXTXE M. ; BILBAO J.** Polyethylene cracking on a spent FCC catalyst in a conical spouted bed. *Ind. Eng. Chem. Res.,* 2012, vol. 51, 14008-14017 **[0091]**
- **ESCHENBACHER A. ; VARGHESE R. J. ; ABBAS-ABADI M. S. ; VAN GEEM K. M.** Maximizing light olefins and aromatics as high value base chemicals via single step catalytic conversion of plastic waste. *Chem. Eng. J.,* 2022, vol. 428, 132087 **[0091]**